e-ISSN: 2550-164X

Available online at
https://jmeche.uitm.edu.my/

Journal of Mechanical Engineering 23(1) 2026, 179 – 211.

Journal of Mechanical Engineering

Predictive Modelling of Hybrid Composite Laminates Buckling Behaviour using Finite Element Analysis, Refined Response Surface Methodology and Artificial Neural Network Models with Different Data Sizes

Muhammad Naufal Mohd Najib[1], Mohd Shahrom Ismail[1], Chi Hieu Le[2], Ho Quang Nguyen[3], Azizul Hakim Samsudin[4*], Jamaluddin Mahmud[1]

[1]*Faculty of Mechanical Engineering, Universiti Teknologi MARA, 40450 Shah Alam, Malaysia*
[2]*Faculty of Science and Engineering, University of Greenwich, Kent, United Kingdom*
[3]*Institute of Engineering and Technology, Thu Dau Mot University, Vietnam*
[4]*Faculty of Mechanical Engineering, Universiti Teknologi MARA, 81750 Masai, Malaysia*

ARTICLE INFO

Article history:
Received 04 November 2025
Revised 10 December 2025
Accepted 19 December 2025
Online first
Published 15 January 2026

Keywords:
Buckling analysis
Hybrid composite laminates
Response surface methodology
Artificial neural network
Statistical significance

DOI:
10.24191/jmeche.v23i1.9426

ABSTRACT

Accurate prediction of buckling loads in composite structures is essential, as their anisotropic and inhomogeneous properties complicate structural analysis. However, traditional predictive models often face limitations such as the inclusion of statistically insignificant polynomial terms in Response Surface Methodology (RSM) and poor learning performance in Artificial Neural Networks (ANN) due to unprocessed and limited data sizes. This study aimed to develop and evaluate predictive models for the buckling load of hybrid graphite/glass epoxy composite laminates using different data sizes. Two datasets were employed, comprising 27 runs generated through a Full Factorial Design (FFD) under the Design of Experiment (DOE) approach and 100 customised experimental runs. Two modelling approaches, RSM and ANN, were employed to predict the buckling load obtained from finite element analysis (FEA). The overall range of computed buckling loads was wide, spanning from 3.627 kN to 1730.8 kN, confirming the strong sensitivity of the structure to the design variables. The highest buckling loads occurred at [45, 1, 3 mm] (angle, volume fraction, thickness), and for hybrid laminates at [45, 0.5, 3 mm]. The RSM predictions produced ratios close to one when compared with FEA results, while the ANN models showed both underprediction and overprediction tendencies. The t-test results indicated no statistically significant difference between the 27 and 100 experimental runs, suggesting that model accuracy was influenced more by modelling approach and data treatment than dataset size. This study may contribute to enhancing knowledge of the buckling behaviour and failure of hybrid graphite/glass composite structures, which will help engineers design safer structures by reducing the risk of buckling.

[4*] Corresponding author. *E-mail address*: azizulhakim@uitm.edu.my
https://doi.org/10.24191/jmeche.v23i1.9426

INTRODUCTION

Composite materials are engineered by combining two or more distinct constituents to create a structure with improved overall performance (Hsissou et al., 2021). They are widely used in aerospace, marine, and automotive applications because of their high strength-to-weight ratio, corrosion resistance, and stiffness (Long et al., 2022). Hybrid composite laminates are formed by stacking different fibre types within a common matrix to balance performance and cost (Suriani et al., 2021). According to Rajak et al. (2021), layering carbon and glass fibres enhances mechanical properties by combining the high strength and stiffness of carbon fibres with the flexibility and impact resistance of glass fibres, resulting in improved structural performance and durability.

The hybridisation of graphite and glass fibres is mainly motivated by cost considerations. Graphite prepregs, priced between $33 and $66 per kilogram, are significantly more expensive than glass prepregs, which cost between $1.3 to $2 per kilogram (Barnett et al., 2024; Joshi et al., 2004). To ensure that replacing expensive graphite fibres with glass does not compromise structural integrity, analytical and numerical studies are required to predict mechanical behaviour and optimise the lay-up for cost-effective performance.

Buckling is a critical failure mode in composite laminates and strongly influences the design of aerospace structures subjected to compressive loads (Goel et al., 2021). Buckling occurs when compressive stresses exceed the structural stiffness, causing sudden out-of-plane deformation. Fig 1 demonstrates the buckling behaviour that can be observed in aircraft fuselage panels subjected to compression forces, where visible surface ripples appear along the body. Numerous studies have been devoted to understanding and improving the buckling resistance of hybrid composite laminates.

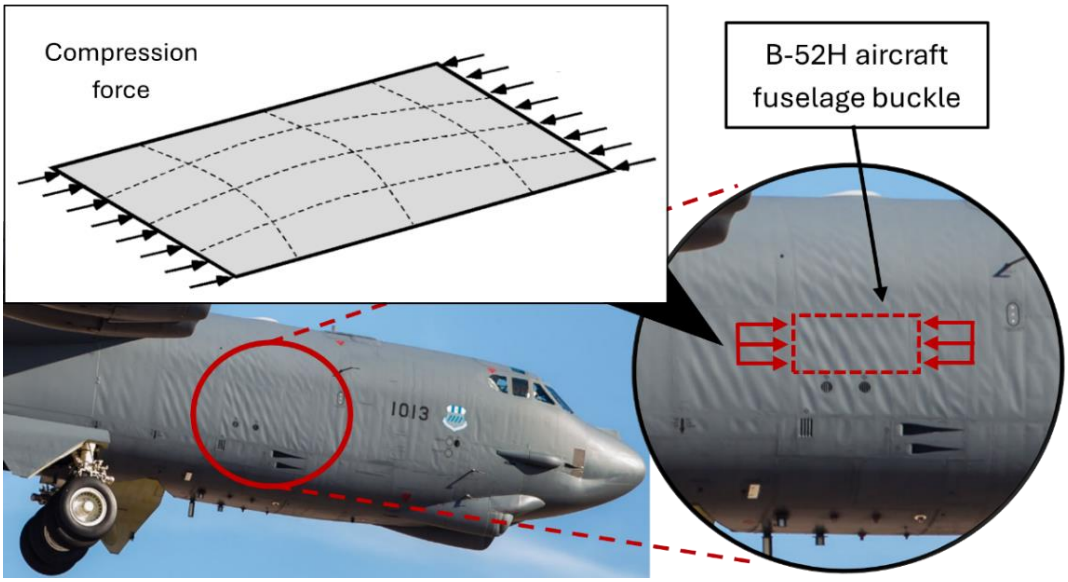

Fig. 1. Buckling behaviour of aircraft body under compression loads (Leishman, 2023).

The dominant approach in buckling analysis of hybrid composite laminates has been Finite Element Analysis (FEA), as demonstrated by Ho-Huu et al. (2016), Kumar et al. (2018), and Achour et al. (2018), who investigated the influence of fibre orientation, stiffener design, plate geometry, and cut-outs on the critical buckling loads. These studies confirmed the flexibility and effectiveness of FEA but also highlighted its reliance on idealised boundary conditions, which may limit its applicability to real structural

https://doi.org/10.24191/jmeche.v23i1.9426

behaviour. Commercial FEA software such as ANSYS (ANSYS, Inc.) provides built-in eigenvalue analysis tools that enable efficient evaluation of complex composite structures. However, FEA models must be validated to ensure accurate physical representation. Studies by Zhang et al. (2025) and Gopalan et al. (2021) validated FEA models through numerical, analytical, and experimental comparisons, improving simulation credibility. Bakamal et al. (2021b) found that carbon nanotube reinforcement enhanced buckling strength and reduced deformation, while Xiao & Harrison (2021) demonstrated that fibre steering increased buckling loads in variable-stiffness laminates. Similarly, Damghani et al. (2021, 2022) highlighted the effects of hybridisation and geometric discontinuities, showing that matrix shear damage mechanisms delay structural failure.

The commonly employed statistical design, optimisation, and predictive models are the Response Surface Methodology (RSM) and Artificial Neural Network (ANN) (Szpisják-Gulyás et al., 2023; Mamun et al., 2020). Optimisation techniques have been widely employed to improve the design of composite laminates. Wang et al. (2019) demonstrated that Discrete Material Optimisation (DMO) effectively optimised stacking sequences and material topology but remained computationally demanding and sensitive to modelling assumptions. Therefore, RSM has emerged as a more practical tool for multi-factor optimisation (Alam et al., 2020). RSM requires the selection of an appropriate statistical design and regression model within a Design of Experiment (DOE) framework (Malekjani & Jafari, 2020), which helps to identify how design factors influence the overall response (Lee et al., 2022).

ANNs have proven effective in pattern recognition and nonlinear data prediction, making them suitable for composite material analysis (Yang et al., 2021). ANN consists of input, hidden, and output neurons connected through weighted links (Thakur & Konde, 2021). The performance of neural networks is influenced by factors such as architecture, training algorithm, and the number of layers (Sarker, 2021). Multilayer Perceptron (MLP) architectures trained with the Levenberg–Marquardt algorithm have been widely used in engineering prediction models (Hemmat et al., 2023; Aghelpour et al., 2022; Can et al., 2022). Kamarudin et al. (2022) and Liu et al. (2023) combined DOE, ANN, and genetic algorithms, showing that advanced modelling techniques can improve prediction accuracy depending on the quality and scope of the training database.

Best practice in predictive modelling combines experimental and numerical approaches to validate results, ensuring accuracy across a wide range of influencing factors. Advanced modelling methods are valuable for capturing the nonlinear behaviour of hybrid laminates. However, experimental methods often struggle to represent the complex relationships among numerous design variables (Reji & Kumar, 2022).

Despite significant progress, research gaps remain in predictive modelling for composite laminates. Limited studies have addressed the effects of data normalisation in ANN and the use of modified polynomial regression functions in RSM, particularly when working with small datasets. The predictive performance of these models is largely affected by their structural formulation and the quality of the dataset (Fan et al., 2021). Furthermore, the combined influence of fibre angle, volume fraction, and plate thickness on the buckling behaviour of hybrid laminates has not been extensively studied.

In terms of the number of input datasets, typical ANN studies utilised thousands of input datasets for network training. Recently, many studies attempted integrating RSM-ANN, where the input datasets for network training were based on the standard 17 runs (input datasets) for RSM-Box Behnken Design model (Okpalaeke et al., 2020; Sibiya et al. 2022; Zhang et al., 2020) and the standard 27 runs (input datasets) RSM-Full Factorial Design model (Ponticelli et al., 2024; Shokri et al., 2020; Saha et al., 2024) or RSM-Central Composite Design model (Santhosh et al., 2021; Silva et al., 2024; Oza et al., 2022) for analysing three factors and three levels cases. The recent outcomes from these studies prove that when integrating RSM and ANN, smaller input datasets could also produce predictive models with reasonable accuracy, thus reducing the dependency on doing experiments with thousands of specimens or performing simulations with thousands of FEA models. For this, this finding could save cost and time from the need to collect massive input data, either from conducting experiments and performing simulations.

https://doi.org/10.24191/jmeche.v23i1.9426

To address the above-mentioned challenges and discussed research gaps regarding predictive modelling for composite laminates, this study aims to develop and evaluate predictive models for the buckling load of hybrid graphite/glass epoxy composite laminates using FEA and refined RSM and ANN models with different data sizes. The study applies model refinement in RSM and a data normalisation approach in ANN to enhance prediction accuracy. Additionally, it seeks to improve the understanding of how the combined effects of fibre orientation, volume fraction, and plate thickness influence the buckling behaviour of hybrid composite laminates.

While earlier studies demonstrated that RSM-ANN integration can work with small datasets, the present study extends this understanding in three keyways. Unlike previous RSM-ANN studies that used standard quadratic models, this work employs a refined fifth order RSM formulation with insignificant terms removed based on statistical screening. This refinement improves prediction stability for nonlinear buckling behaviour while avoiding over-parameterisation. The ANN in this study applies min-max data normalisation before training. This treatment reduces scale imbalance among the inputs and enhances convergence, which is not fully explored in earlier composite-buckling ANN studies. Another contribution of this work is the direct comparison between 27 and 100 experimental runs, supported by independent t-tests. This analysis quantitatively shows how dataset size influences the performance of refined RSM and normalised ANN models, which has not been reported in previous hybrid RSM-ANN applications. Together, these refinements provide new insight into how small, statistically designed datasets can still produce accurate buckling predictions when combined with appropriate data treatment and model reduction. The results also establish that increasing the dataset size beyond statistically designed levels does not significantly improve mean prediction accuracy, offering practical guidance for reducing computational and experimental workload.

METHODOLOGY

In this study, FEA was conducted to determine the buckling load of hybrid graphite/glass epoxy composite laminates using ANSYS Mechanical APDL (Version 16.0, 2014, SAS IP, Inc.). The simulations were designed using a Full Factorial Design (FFD) within the DOE framework. Data obtained from FEA was used to develop predictive models using RSM in Design-Expert Software (Version 22.0.6, Stat-Ease, Inc.) and ANN in MATLAB (Version R2017b, The MathWorks, Inc.). The RSM and ANN results were then compared with FEA outputs, followed by a t-test to confirm statistical consistency.

Mesh convergence analysis and FE model validation

The mesh convergence analysis and numerical validation were performed using a reference model from Phan & Reddy (1985). The analysis employed the Shell 281 element type with mesh sizes ranging from 2 × 2 to 100 × 100. A square plate model with dimensions of $a = 1$ m and $h = 0.1$ m, and a lamination sequence of [0, 90, 90, 0] was used. Table 1 shows idealised properties for the validation model, created by varying the orthotropy ratio. A simply supported boundary condition (Fig 2(a)) and a 1000 N/m uniaxial compressive load along the x-axis (Fig (2b)) were applied. The mesh convergence results were evaluated using the non-dimensional buckling load derived from Equation 1, where the eigenvalue was obtained directly from the simulation. The FEA model validation used the same geometry, material properties, boundary conditions, and loading as in the mesh convergence analysis, but the mesh size was adjusted to 20 × 20, matching Phan & Reddy (1985). Validation employed the non-dimensional buckling load derived from Equation 1, with the eigenvalue obtained directly from the simulation.

$$\lambda = \overline{N_x}\frac{a^2}{E_2 h^2} \tag{1}$$

https://doi.org/10.24191/jmeche.v23i1.9426

Table 1. Material properties according to orthotropy

E_1/E_2	3	10	20	30	40
E_1	40 GPa	40 GPa	40 GPa	40 GPa	40 GPa
E_2	13.3 GPa	4 GPa	2 GPa	1.33 GPa	1 GPa
$G_{12} = G_{13}$	8 GPa	2.4 GPa	1.2 GPa	800 MPa	600 MPa
G_{23}	6.67 GPa	2 GPa	1 GPa	667 MPa	500 MPa

Source: (Phan & Reddy, 1985)

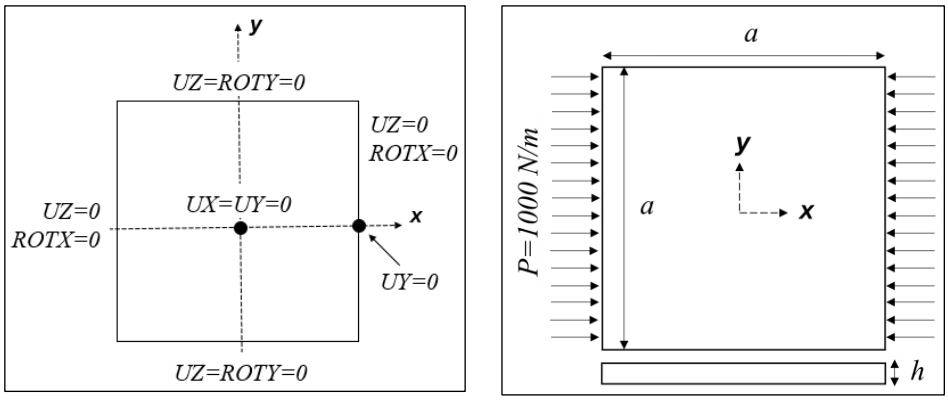

Fig. 2. Schematic diagram for (a) simply supported boundary condition and (b) loading condition with plate dimensions.

Key factors influencing the buckling behaviour of hybrid composites

Two case studies were developed using a DOE approach to examine the influence of key factors on the buckling behaviour of hybrid composites. The first case study employed a three-level FFD consisting of 27 experimental runs, representing all combinations of the three input factors. The second case study increased the number of experimental runs by adding intermediate factor levels between the original three levels, resulting in five levels for each factor. The design was based on a Box–Behnken Design (BBD), and this approach produced almost 100 datasets for simulation. Among these runs, 20 repeated runs were included as centre-point designs to provide balanced coverage of the factor space and support regression analysis. The selected factors were volume fraction (0, 0.5, and 1), angle of orientation (0° to 45°), and plate thickness (0.0005 m to 0.003 m). The angle of orientation was applied to the fibre direction of both glass/epoxy and graphite/epoxy layers, since all layers in the hybrid laminate were given the same orientation. The volume fractions '0', '0.5', and '1' correspond to 100% glass/epoxy laminate, 50% glass/epoxy and 50% graphite/epoxy laminate, and 100% graphite/epoxy laminate, respectively. The detailed factor settings are presented in Table 2.

Table 2. Design factors set up

Factor	Unit	Low	High
Angle of Orientation	∘	0	45
Volume Fraction	unitless	0	1
Plate Thickness	m	0.0005	0.003

https://doi.org/10.24191/jmeche.v23i1.9426

Determination of the buckling load of hybrid composites using FEA

The buckling load of hybrid graphite/glass epoxy composite laminates is determined through FEA simulation. A square plate model with dimensions of 0.05 m × 0.05 m and a lamination sequence of [0/+θ/−θ/90]s was used for the FEA simulation, as illustrated in Fig 3. Within ANSYS, graphite was assigned as material 1 and glass as material 2. The analysis employed the Shell 281 element type, and the material properties used are listed in Table 3, showing the actual properties of graphite epoxy and glass epoxy for the current FE model. A 20 × 20 mesh size was selected based on the mesh convergence analysis. The boundary and loading conditions followed those shown in Fig 2. A linear buckling analysis was conducted, considering only the first mode shape, which represents the lowest critical buckling load.

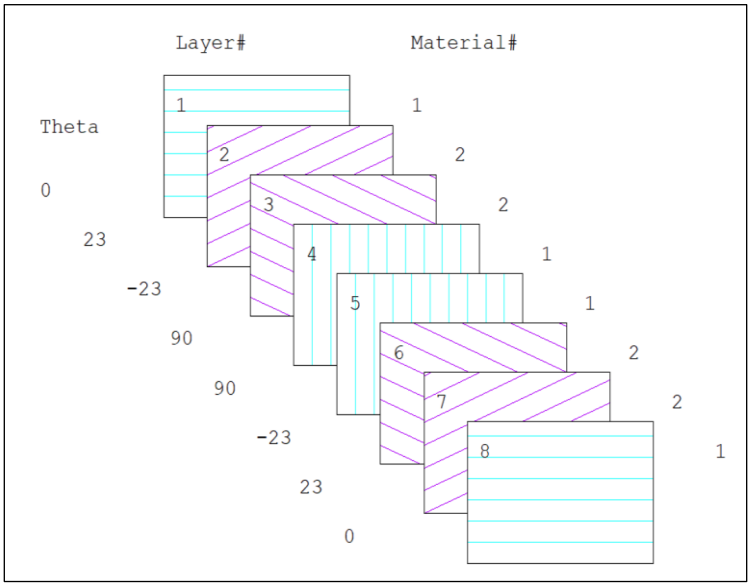

Fig. 3. Layer sequence of [0/+θ /-θ /90]s for current study on hybrid composite laminates.

Table 3. Material properties for graphite epoxy and glass epoxy (Dogan, 2020)

Properties	Graphite Epoxy	Glass Epoxy
E_1	132.38 GPa	44.93 GPa
$E_2 = E_3$	10.76 GPa	14.04 GPa
$V_{12} = V_{13} = V_{23}$	0.25	0.2481
$G_{12} = G_{13}$	5.56 GPa	5.26 GPa
G_{23}	3.38 GPa	5.10 GPa
Density	1605 kg/m^3	2081 kg/m^3

Prediction of the buckling load based on RSM and ANN

Two modelling approaches, RSM and ANN, were employed to predict the buckling load obtained from FEA. The RSM models were developed using modified regression functions by removing terms with a p-value higher than 0.05 from the fifth-order polynomial structure. The initial statistical polynomial model was fifth order, but ANOVA (RSM) indicated that some terms were insignificant and should be removed. This led to a simpler equation with better predictive accuracy that resulted in the modified regression

https://doi.org/10.24191/jmeche.v23i1.9426

functions. Based on the Design of Experiment (DOE) data, two RSM models were created using ANOVA. The first model, RSM-27, was developed from the DOE containing 27 experimental runs. The second model, RSM-100, was generated using 100 experimental runs and applied the same regression function as RSM-27 for direct comparison.

The ANN models were developed using normalised datasets, where all input factors (angle of orientation, volume fraction, and plate thickness) and the output buckling load were scaled to a range between 0 and 1. The normalisation was performed using the min-max method, as shown in Equation 2, where the original data value $x'$was transformed into the normalised value $x_i$using the minimum and maximum values of each feature (Aksu et al., 2019). The ANN models were developed in MATLAB using a MLP architecture with three inputs, ten neurons in the hidden layer, and one output as shown in Fig 4. The models were trained using the Levenberg–Marquardt (LM) algorithm due to its rapid convergence and stability with medium-sized networks (Revanesh et al., 2024). A tangent sigmoid activation function, defined in Equation 3, was applied to the input neurons for its effectiveness in regression tasks (Adizue & Takács, 2025; Hajduk & Dec, 2023). Two ANN models were developed where ANN-27, based on the DOE with 27 experimental runs, and ANN-100 with 100 experimental runs.

$$x' = \frac{x_i - min}{max - min} \tag{2}$$

$$f(x) = \frac{2}{1 + e^{-2x}} \tag{3}$$

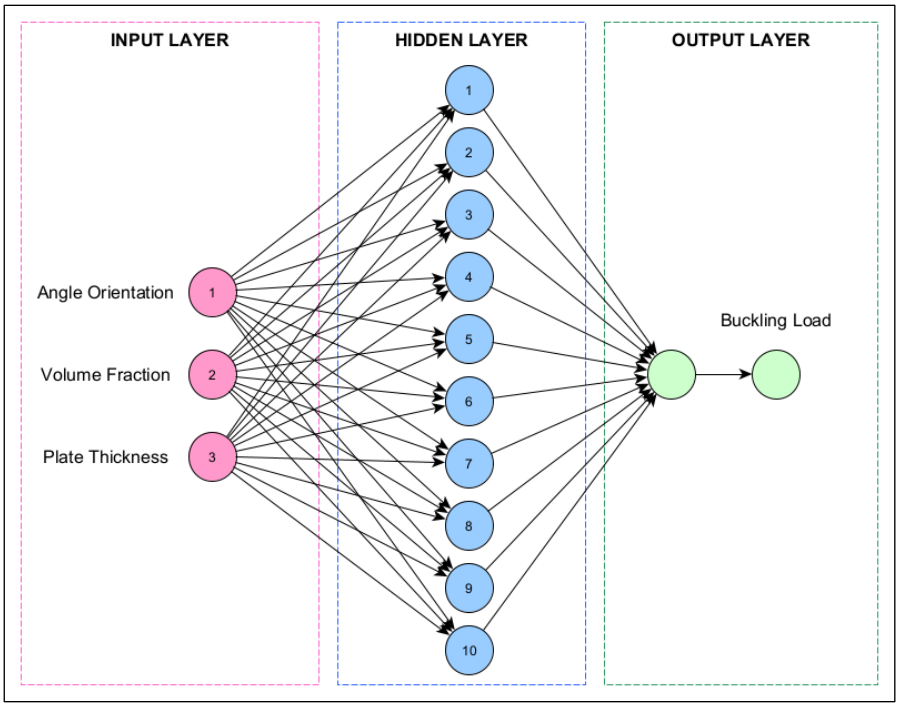

Fig. 4. Multilayer perceptron (MLP) employed in this study.

https://doi.org/10.24191/jmeche.v23i1.9426

RESULTS AND DISCUSSION

Selected mesh size for FEA models

Fig 5 presents the mesh convergence graph for the non-dimensional buckling load at different orthotropy ratios. The graph shows that as the mesh size increases, the buckling load experiences initial fluctuations before stabilising at larger mesh sizes. This trend is consistent with the findings of Evran (2020) and Okereke & Keates (2018). The selected mesh size for the finite element model in the current study is 20 × 20, as higher mesh densities were found to increase computational time without improving accuracy. This conclusion agrees with Gukop et al. (2021) and Bijjam et al. (2023), who reported that excessive mesh refinement significantly increases computing time but has minimal impact on stress or buckling accuracy. Therefore, the minimum mesh of 16 × 16 was found to be sufficient; however, a 20 × 20 mesh was selected to allow for tolerance, as further increases in mesh density significantly raised computational time. This choice also followed Phan & Reddy (1985), as the mesh convergence analysis confirmed that their 20 × 20 mesh was fully converged, justifying its use in this study.

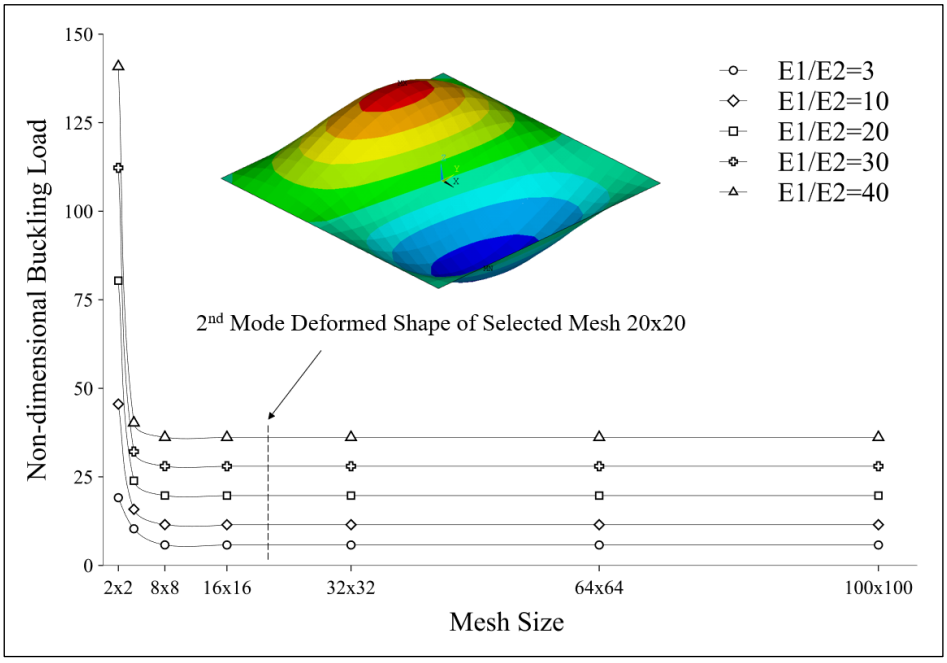

Fig. 5. Mesh convergence graph on non-dimensional buckling load with deformed shaped of selected mesh.

Buckling load determination and validation

Table 4 presents the comparison of non-dimensional buckling loads between the results from Phan & Reddy (1985) and the current study. The error between the ANSYS predictions and the Classical Laminate Plate Theory (CLPT) values was less than 5%, ranging from 0.001% to 0.23%. The lower buckling loads predicted by the Higher-Order Shear Deformation Theory (HSDT) reflect its inclusion of shear deformation effects, which reduce the overall stiffness of the laminate, as reported by Li et al. (2020) and Schilling & Mittelstedt (2025). These results confirm that the FEA predictions were consistent with the reference models, validating the accuracy of the developed FEA model.

https://doi.org/10.24191/jmeche.v23i1.9426

Table 4. Comparison results between present and past studies

Orthotropy ratio (E1/E2)	Method			Error (%) |A – B| / A x 100
	HSDT (Phan & Reddy, 1985)	CLPT (Phan & Reddy, 1985) (A)	Current (ANSYS) (B)	
3	5.1143	5.7538	5.7647	0.19
10	9.774	11.492	11.4916	0.003
20	15.298	19.712	19.7118	0.001
30	19.957	27.936	28.0012	0.23
40	23.34	36.16	36.1576	0.007

Table 5 presents the FEA results together with the corresponding design factors, where the buckling load ranged between 3.627 kN and 1730.8 kN. Fig 6 shows the influence of design factors on the buckling load, where additional data points were interpolated between factor values from the 100 experimental runs. The results indicate that laminates oriented at 45° tend to exhibit higher buckling loads, which aligns with the findings of Phan & Reddy (1985), Alhawamdeh et al. (2021), and Rostamijavanani et al. (2021), who reported that fibres aligned close to 45° distribute in-plane loads more effectively, enhancing stiffness and buckling resistance. An increase in graphite content was also found to raise the buckling load, consistent with Bakamal et al. (2021a) and Han & Dong (2024), who observed that laminates with higher graphite fibre content exhibit superior buckling performance due to an increase in in-plane stiffness. Furthermore, increasing plate thickness was shown to significantly increase the buckling load, in agreement with Wankhade & Niyogi (2020), Silva & Meddaikar (2020), and Yang et al. (2022), who demonstrated that thicker plates possess higher bending stiffness and greater resistance to buckling. Fig 7 illustrates a contour plot of modes 1–3 for the configuration that produced the highest buckling load, where the mode shapes represent the buckling deformation patterns and corresponding buckling load factor values after load application. Overall, the results confirm that fibre orientation, graphite content, and plate thickness strongly influence the buckling behaviour of hybrid composite laminates.

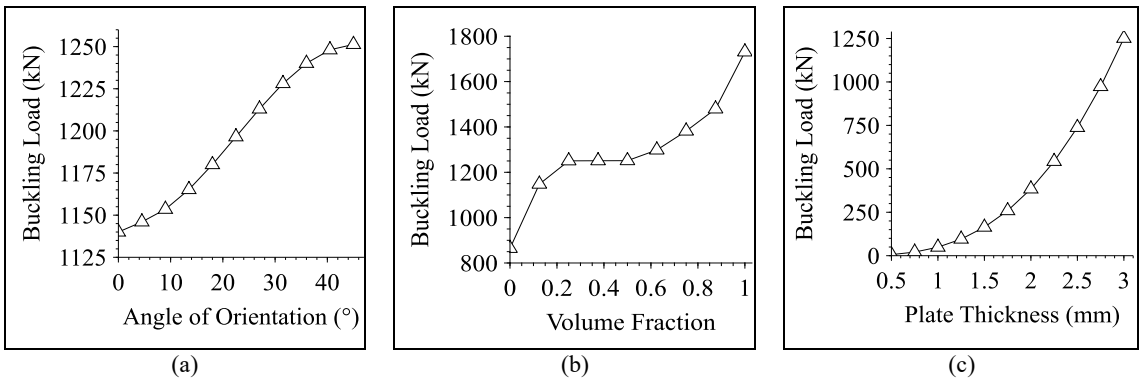

Fig. 6. Influence of design factors on buckling load for (a) angle of orientation, (b) volume fraction and (c) plate thickness.

https://doi.org/10.24191/jmeche.v23i1.9426

Table 5. Buckling load from ANSYS for FFD factors setup

Run	Angle of orientation (°)	Volume fraction	Plate thickness (m)	FEA-ANSYS (kN)
1	0	1	0.003	1382.2
2	0	0	0.0005	3.627
3	22.5	0.5	0.00175	248.72
4	0	0.5	0.003	1143.4
5	22.5	1	0.003	1555.8
6	45	1	0.00175	365.61
7	45	0	0.003	864.33
8	45	1	0.003	1730.8
9	45	0	0.00175	175.47
10	22.5	0.5	0.003	1196.5
11	22.5	0	0.003	811.23
12	0	1	0.0005	7.0333
13	0	0.5	0.00175	237.14
14	22.5	1	0.0005	7.9143
15	0	0	0.00175	153.89
16	45	1	0.0005	8.7967
17	45	0.5	0.0005	6.1688
18	0	0	0.003	758.56
19	0	1	0.00175	292.2
20	22.5	0	0.00175	164.65
21	45	0.5	0.003	1251.3
22	22.5	0	0.0005	3.8817
23	22.5	1	0.00175	328.84
24	22.5	0.5	0.0005	5.9109
25	45	0.5	0.00175	259.07
26	0	0.5	0.0005	5.6518
27	45	0	0.0005	4.1371

Note: Buckling load for 100 experimental runs in appendix A.

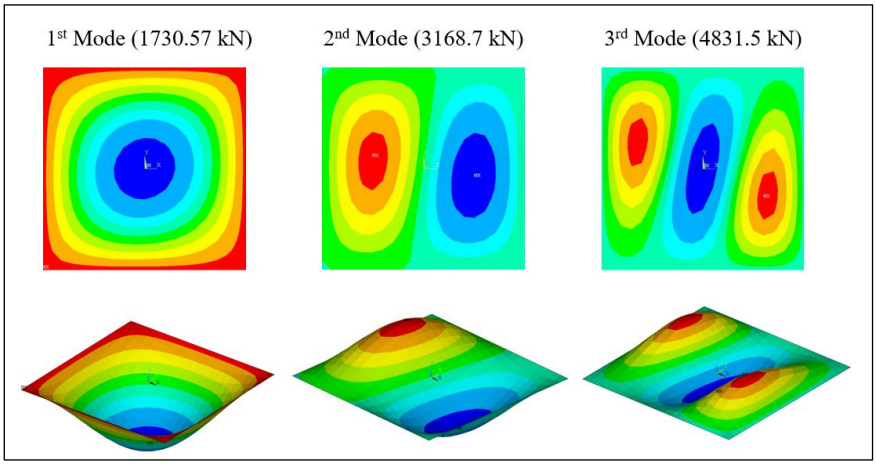

Fig. 7. Contour plot of modes 1-3 under high buckling loads.

https://doi.org/10.24191/jmeche.v23i1.9426

ANOVA-based RSM model evaluation results

Model significance

Table 6 presents the ANOVA results for the RSM models. The results show that the models were highly significant, with very low p-values, where the highest recorded value was 0.0002. This finding aligns with Khelifa et al. (2025) and Sibiya et al. (2022), who stated that factors with p-values below 0.05 are considered statistically significant, indicating that the regression function effectively explains most variations in the response variable. Table 7 presents the fit statistics for the RSM models, highlighting the R^2, Adjusted R^2, and Predicted R^2 values, all of which were close to 1. According to Kumar et al. (2023), such values demonstrate excellent model performance and strong predictive accuracy for both known and unseen data. Additionally, the R^2 values being close to the Adjusted R^2 values confirm the overall significance and stability of the model, consistent with Boukarma et al. (2023).

Table 6. ANOVA for statistical design models

Source	Network Model				
	Sum of squares	df	Mean square	F-value	p-value
Model	7.973E+12	17	4.690E+11	3.856E+06	< 0.0001
A-Angle of orientation	2.405E+08	1	2.405E+08	1976.91	< 0.0001
B-Volume fraction	4.045E+10	1	4.045E+10	3.325E+05	< 0.0001
C-Plate thickness	2.128E+12	1	2.128E+12	1.75E+07	< 0.0001
AB	6.716E+08	1	6.716E+08	5521.32	< 0.0001
AC	2.883E+09	1	2.883E+09	23700.18	< 0.0001
BC	4.117E+11	1	4.117E+11	3.384E+06	< 0.0001
B^2	4.702E+06	1	4.702E+06	38.66	0.0002
C^2	2.495E+11	1	2.495E+11	2.051E+06	< 0.0001
ABC	7.295E+09	1	7.295E+09	59973.67	< 0.0001
AB^2	2.179E+08	1	2.179E+08	1791.06	< 0.0001
AC^2	3.473E+08	1	3.473E+08	2855.26	< 0.0001
B^2C	1.752E+08	1	1.752E+08	1439.98	< 0.0001
BC^2	4.420E+10	1	4.420E+10	3.634E+05	< 0.0001
AB^2C	2.347E+09	1	2.347E+09	19294.63	< 0.0001
ABC^2	8.216E+08	1	8.216E+08	6754.72	< 0.0001
B^2C^2	3.463E+07	1	3.463E+07	284.68	< 0.0001
AB^2C^2	2.628E+08	1	2.628E+08	2160.36	< 0.0001
Residual	1.095E+06	9	1.216E+05		
Cor total	7.973E+12	26			

Table 7. Fit statistics for statistical design models

Model evaluation metrics	Network model
Standard deviation	348.76
Coefficient of variation (%)	0.0726
Coefficient of determination (R^2)	1.0000
Adjusted R^2	1.0000
Predicted R^2	1.0000
Adequate precision	6064.4733

https://doi.org/10.24191/jmeche.v23i1.9426

Regression functions

Equation 4 presents the regression functions developed from the reduced fifth-order polynomial model. The coefficients in these equations indicate how each factor—Angle of Orientation (A), Volume Fraction (B), and Plate Thickness (C)—individually influences the buckling behaviour. Positive coefficients represent a beneficial effect of the respective factor on the buckling load, while negative coefficients indicate an adverse influence, as explained by Boukarma et al. (2023). Using these regression functions, the predicted buckling loads for both RSM-27 and RSM-100 models can be calculated, allowing estimation of the buckling response across the defined design space.

$$\begin{aligned} P_{cr} = {} & 70745.09733 + 216.79484A + 76356.996B - 206933000C - 427.84836AB \\ & - 635346AC - 227902000BC - 28827.07467B^2 \\ & + 145394000000C^2 + 1280070ABC + 879.87378AB^2 \\ & + 448854000AC^2 + 83608800B^2C + 169154000000BC^2 \\ & - 2627700AB^2C - 957694000ABC^2 - 57061800000B^2C^2 \\ & + 1956260000AB^2C^2 \end{aligned} \quad (4)$$

Residuals

Fig 8 presents the normal plot of residuals and the residuals versus predicted plot for the RSM-27 model. Fig 8(a) shows that the residuals cluster closely along the fitted line, indicating that the residuals are normally distributed, which confirms the adequacy of the model according to Feng et al. (2020). In Fig 8(b), the dashed lines represent the control limits (±4.16) for the externally studentised residuals. The data points are well distributed within these limits, demonstrating that no significant outliers exist and that the model exhibits consistent variance across the predicted values. These results verify that the regression assumptions were satisfied and that the RSM-27 model provides a reliable fit to the data.

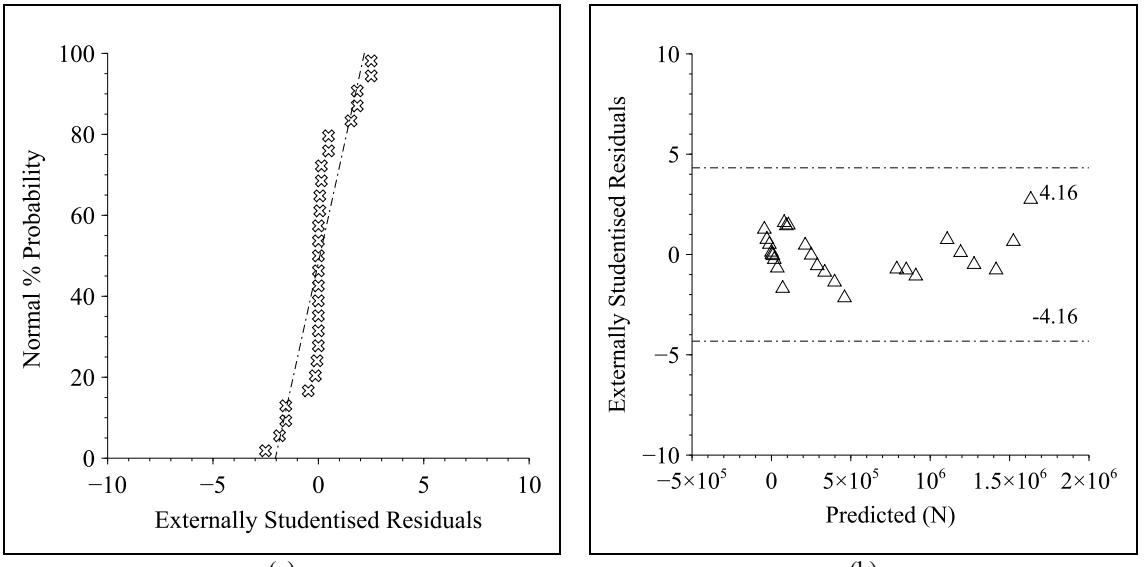

Fig. 8. (a) Normal plot of residuals and (b) residuals vs predicted for RSM-27 model.

https://doi.org/10.24191/jmeche.v23i1.9426

Factor interaction and contour plots

Figs 9 to 14 present the three-dimensional surface contour plots illustrating the interactions between the design factors for both RSM-27 and RSM-100 models. The plot is color-coded from blue (lower buckling load) to red (higher buckling load). The three factors considered were the angle of orientation, A (°), the volume fraction, B, and the plate thickness, C (m). The results indicate that plate thickness had the strongest effect on the buckling load, as shown by the steep gradients along the thickness axis. Increasing plate thickness significantly increased the buckling load, confirming its dominant role in enhancing stiffness and improving structural stability. The angle of orientation exhibited a moderate influence compared with thickness. The plots showed that laminates oriented near 45° tended to produce higher buckling loads, consistent with the trends observed in the FEA results. The influence of volume fraction was also noticeable, with higher graphite content increasing the buckling load, particularly at greater plate thicknesses. However, the interaction between volume fraction and angle of orientation was weak, as indicated by relatively flat contour patterns. Overall, the interaction plots confirmed that plate thickness, followed by graphite volume fraction and fibre orientation, are the key factors influencing the buckling behaviour of hybrid composite laminates.

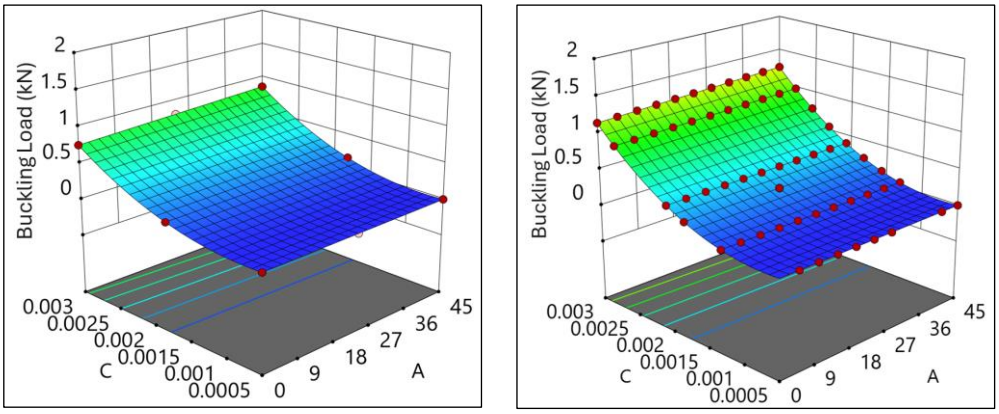

Fig. 9. Interaction between factor A and C in 3D contour plot for (a) RSM-27 and (b) RSM-100.

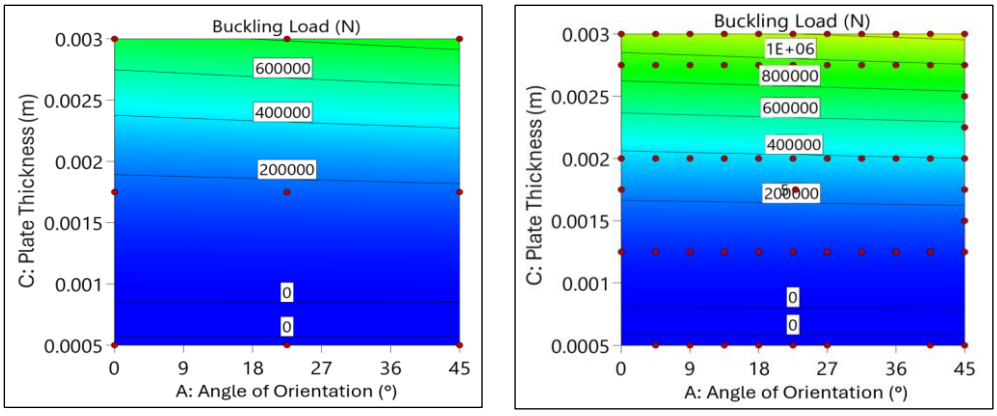

Fig. 10. Interaction between factor A and C in contour plot for (a) RSM-27 and (b) RSM-100.

https://doi.org/10.24191/jmeche.v23i1.9426

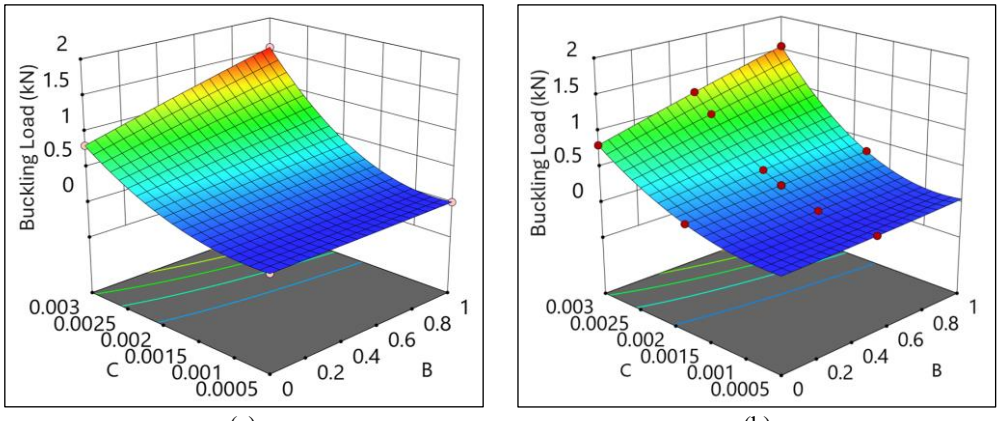

(a) (b)

Fig. 11. Interaction between factor B and C 3D contour plot for (a) RSM-27 and (b) RSM-100.

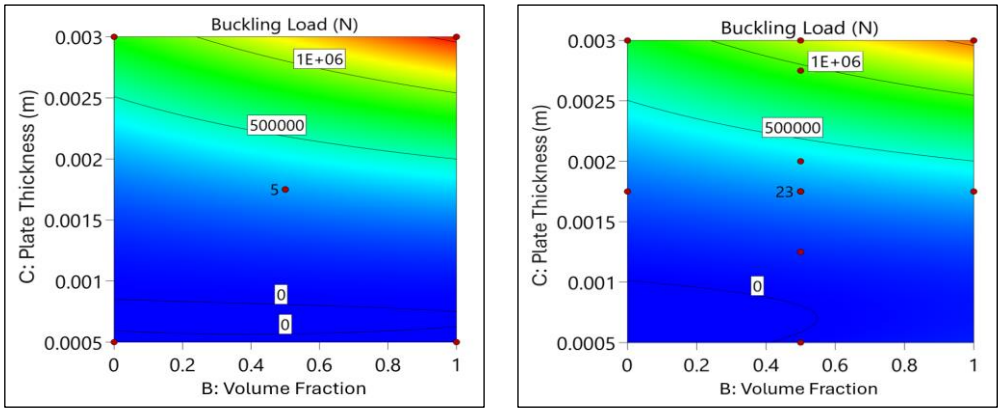

(a) (b)

Fig. 12. Interaction between factor B and C in contour plot for (a) RSM-27 and (b) RSM-100.

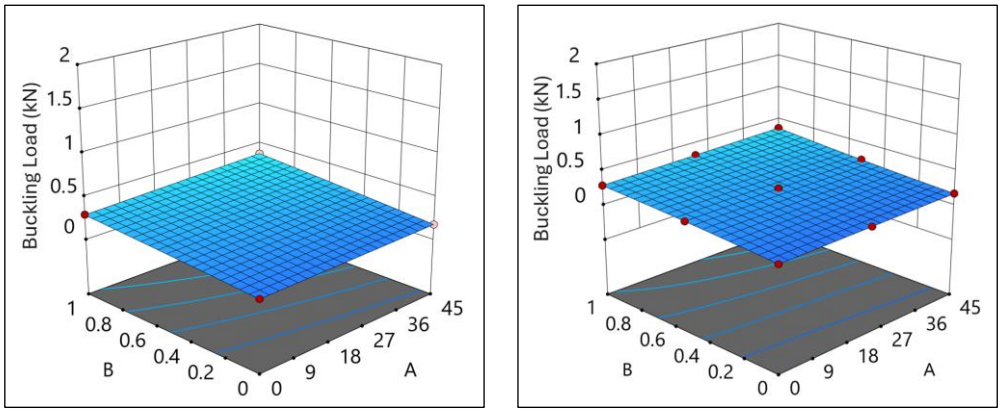

(a) (b)

Fig. 13. Interaction between factor A and B in 3D contour plot for (a) RSM-27 and (b) RSM-100.

https://doi.org/10.24191/jmeche.v23i1.9426

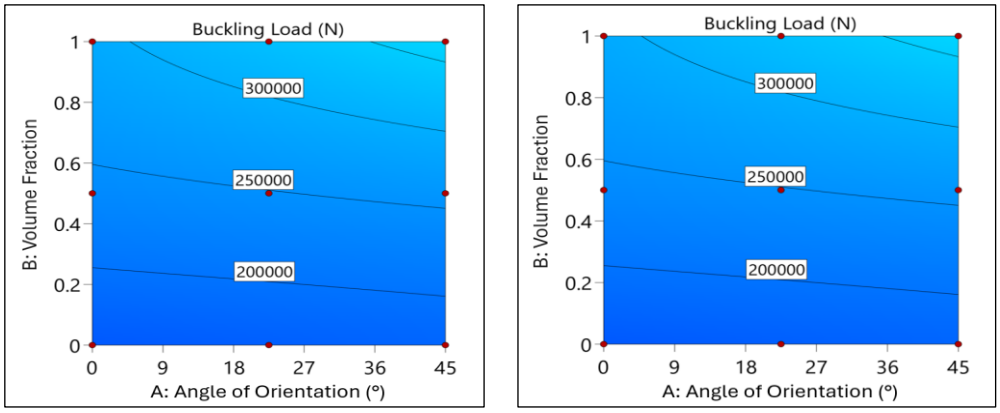

Fig. 14. Interaction between factor A and B in contour plot for (a) RSM-27 and (b) RSM-100.

ANN models performance

For the ANN models, the dataset was divided into three subsets consisting of 70% for training, 15% for validation, and 15% for testing. For the ANN-27 model, this split corresponded to 19 samples for training, 4 for validation, and 4 for testing. For the ANN-100 model, 70 samples were used for training, with 15 each for validation and testing. The training results are summarised in Table 8. The results show that the ANN-100 model achieved higher correlation coefficients (R) during both validation and testing phases compared with ANN-27, with R values closer to 1, indicating stronger predictive performance and better generalisation. Additionally, the ANN-100 model produced a lower mean square error (MSE) than ANN-27, demonstrating improved accuracy and stability. Overall, the results confirmed that increasing the dataset size enhanced the ANN model's learning capability, yielding more accurate and reliable buckling load predictions.

Table 8. Training results for ANN models

Type	ANN-27		ANN-100	
	MSE	R	MSE	R
Training	0.0000	1.0000	6.1386e-6	0.99998
Validation	0.0032	0.9992	2.7637e-5	0.99985
Test	0.0038	0.99737	2.2763e-65	0.99987

Regression results

Fig 15 presents the regression plots showing the relationship between the predicted (output) and actual (target) buckling loads for the datasets. The dotted line represents the ideal line where the output (Y) = target for a perfect fit (T). The findings show an overall fit (All R-value) of 0.99936 for the ANN-27 model and 0.99994 for the ANN-100 model, indicating a very strong correlation between predicted and actual values. Both models demonstrated excellent performance across all subsets, with data points tightly clustered along the fit line, suggesting that the predictions were highly consistent with the actual targets, as stated by Ertugrul et al. (2025). When comparing both models, the ANN-100 model exhibited a stronger regression alignment across all subsets, showing minimal deviation from the fit line compared with ANN-27.

https://doi.org/10.24191/jmeche.v23i1.9426

Network validation results

Fig 16 shows the performance plots of the ANN models, illustrating the MSE value across different epochs for the training, validation, and testing datasets. The results indicate that the ANN-100 model achieved a slightly lower MSE value for the validation best line (green dotted line) compared with the ANN-27 model, demonstrating better overall accuracy and generalisation. The ANN-27 model reached its minimum validation error at epoch 7, while the ANN-100 model at epoch 10. According to Roy et al. (2021), a smaller number of epochs indicates a faster learning cycle. Although a higher epoch count reflects more training iterations required to reach optimal performance due to data complexity, it does not negatively affect model accuracy, as reported by Afaq & Rao (2020). Overall, both models performed well, with ANN-100 showing improved stability and convergence efficiency compared with ANN-27.

Distribution of prediction error

Fig 17 shows the error histogram plots that categorise the error between the predicted and actual buckling loads into 20 bins. The results indicate that the ANN-100 model exhibited a narrower error range, with values between −0.008 and +0.01, compared with the ANN-27 model, which ranged from −0.01 to +0.04. Although the ANN-27 model displayed a tighter error distribution across all datasets, the wider error range reduced its overall prediction precision. In contrast, the ANN-100 model produced smaller errors and demonstrated greater consistency and accuracy across all datasets. This finding aligns with Chakravarty et al. (2020), who reported that when most prediction errors are concentrated near zero, and only a few outliers are present, it indicates that the ANN model has effectively learned the data patterns. Overall, the results confirm that both models performed well, with the ANN-100 model achieved higher predictive reliability and generalisation performance than the ANN-27 model.

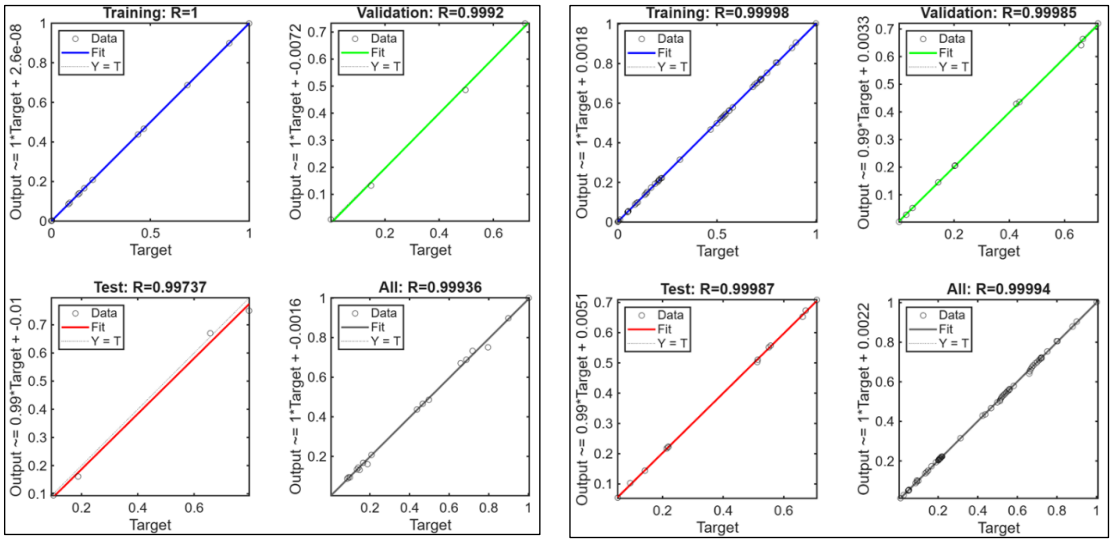

(a) (b)

Fig. 15. Regression plot for (a) ANN-27 and (b) ANN-100.

https://doi.org/10.24191/jmeche.v23i1.9426

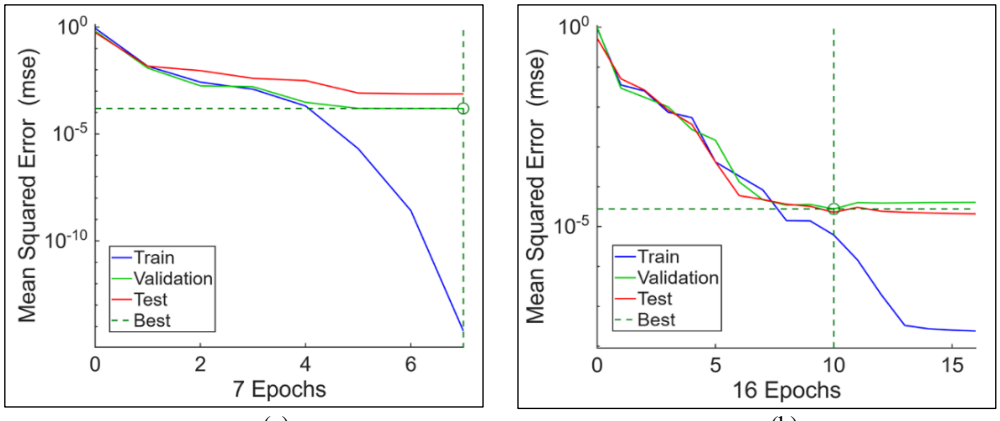

(a) (b)

Fig. 16. Performance plot for (a) ANN-27 and (b) ANN-100.

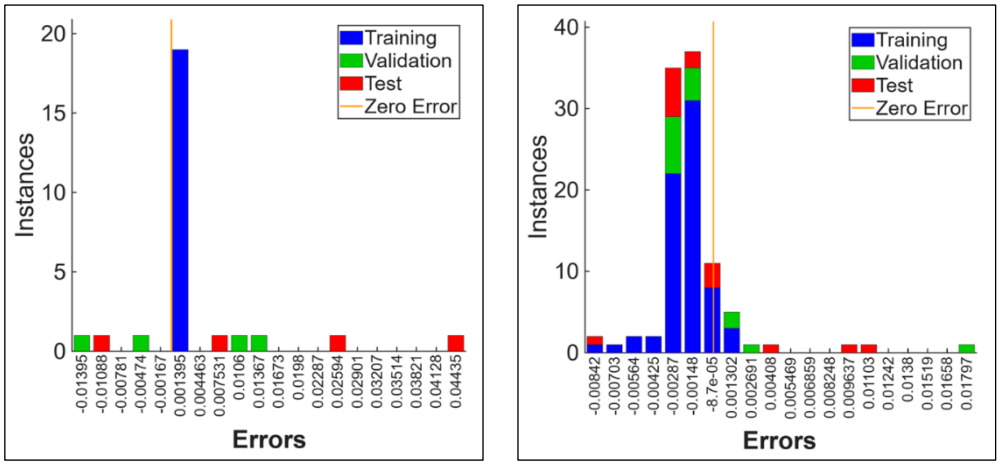

(a) (b)

Fig. 17. Error histogram plot for (a) ANN-27 and (b) ANN-100.

Results comparison of predictive models

Table 9 compares the predicted buckling loads and percentage errors obtained from the RSM and ANN models against the FEA results for the 27 experimental runs. The full comparison for all 100 experimental runs with FEA results is presented in Appendix B. The data in Table 9 are further visualised in Fig 18, which illustrates that both predictive models closely followed the same trend as the FEA results across most experimental runs, demonstrating their reliability in capturing the overall buckling behaviour. Figs 19 and 20 present the ratio of the predicted buckling loads obtained from the RSM and ANN models to the corresponding FEA results for all lamination combinations. The ratio represents the level of agreement between the predictive and numerical results.

In Figs 19 and 20, both RSM-27 and RSM-100 models produced ratios very close to one (unity), showing excellent consistency with the FEA predictions across all lamination combinations. The RSM-100 model demonstrated slightly better accuracy than RSM-27, reflecting the benefit of a larger dataset in improving regression precision. These results confirm that the RSM approach provided stable and reliable predictions of buckling loads within the studied design range.

https://doi.org/10.24191/jmeche.v23i1.9426

Fig 20 shows that the ANN models exhibited greater variation in the ratios compared with FEA results. The ANN-100 model displayed improved alignment with FEA compared with ANN-27, although several lamination combinations showed deviations, with ratios above 1.1 or below 0.9. This indicates that the ANN predictions were more sensitive to data variation and model training quality. This behaviour occurs because RSM relies on a fixed regression equation derived from the experimental design, making its predictions less affected by small variations in the dataset, whereas ANN learns patterns directly from the data, so its performance strongly depends on the size, quality, and distribution of the training dataset (Jha & Sit, 2021). Overall, the RSM models offered more consistent performance, while the ANN models provided adaptable but data-dependent accuracy, improving notably with increased dataset size.

Table 9. Predicted buckling load from ANSYS, RSM and ANN models for 27 experimental runs

FEA-ANSYS (A)	Response (kN)				Error percentage (%)			
	RSM-27 (B)	RSM-100 (C)	ANN-27 (D)	ANN-100 (E)	|A – B| / A x 100	|A – C| / A x 100	|A – D| / A x 100	|A – E| / A x 100
1381.97	1381.97	1381.97	1299.35	1395.73	0.0	0.0	6.0	1.0
3.63	3.63	3.63	3.63	4.55	0.0	0.0	0.0	25.5
248.72	248.31	248.31	248.71	252.86	0.2	0.2	0.0	1.7
1143.12	1143.12	1143.12	1161.70	1111.09	0.0	0.0	1.6	2.8
1556.27	1556.27	1556.27	1554.28	1566.72	0.0	0.0	0.1	0.7
365.59	365.59	365.59	362.71	372.90	0.0	0.0	0.8	2.0
864.26	864.26	864.26	843.55	862.20	0.0	0.0	2.4	0.2
1730.57	1730.57	1730.57	1730.80	1737.71	0.0	0.0	0.0	0.4
175.46	175.46	175.46	164.72	174.01	0.0	0.0	6.1	0.8
1197.07	1197.07	1197.07	1191.92	1199.18	0.0	0.0	0.4	0.2
811.38	811.38	811.38	809.53	811.77	0.0	0.0	0.2	0.1
7.03	7.03	7.03	7.08	6.98	0.0	0.0	0.7	0.7
237.14	237.35	237.35	236.45	239.90	0.1	0.1	0.3	1.2
7.92	7.92	7.92	7.25	7.86	0.0	0.0	8.3	0.7
153.88	153.88	153.88	153.20	154.37	0.0	0.0	0.4	0.3
8.80	8.80	8.80	8.64	10.72	0.0	0.0	1.8	21.8
6.17	6.17	6.17	6.39	8.21	0.0	0.0	3.6	33.2
758.49	758.49	758.49	757.71	755.12	0.0	0.0	0.1	0.5
292.18	292.18	292.18	292.06	304.33	0.0	0.0	0.0	4.2
164.67	164.67	164.67	164.77	180.32	0.0	0.0	0.1	9.5
1251.02	1251.02	1251.02	1269.30	1252.03	0.0	0.0	1.4	0.1
3.88	3.88	3.88	3.97	4.23	0.0	0.0	2.3	9.0
328.89	328.89	328.89	282.91	338.35	0.0	0.0	14.0	2.9
5.91	5.91	5.91	6.39	7.65	0.0	0.0	8.1	29.4
259.07	259.28	259.28	233.00	262.53	0.1	0.1	10.1	1.3
5.65	5.65	5.65	6.39	6.98	0.0	0.0	13.1	23.5
4.14	4.14	4.14	4.15	5.16	0.0	0.0	0.2	24.7

https://doi.org/10.24191/jmeche.v23i1.9426

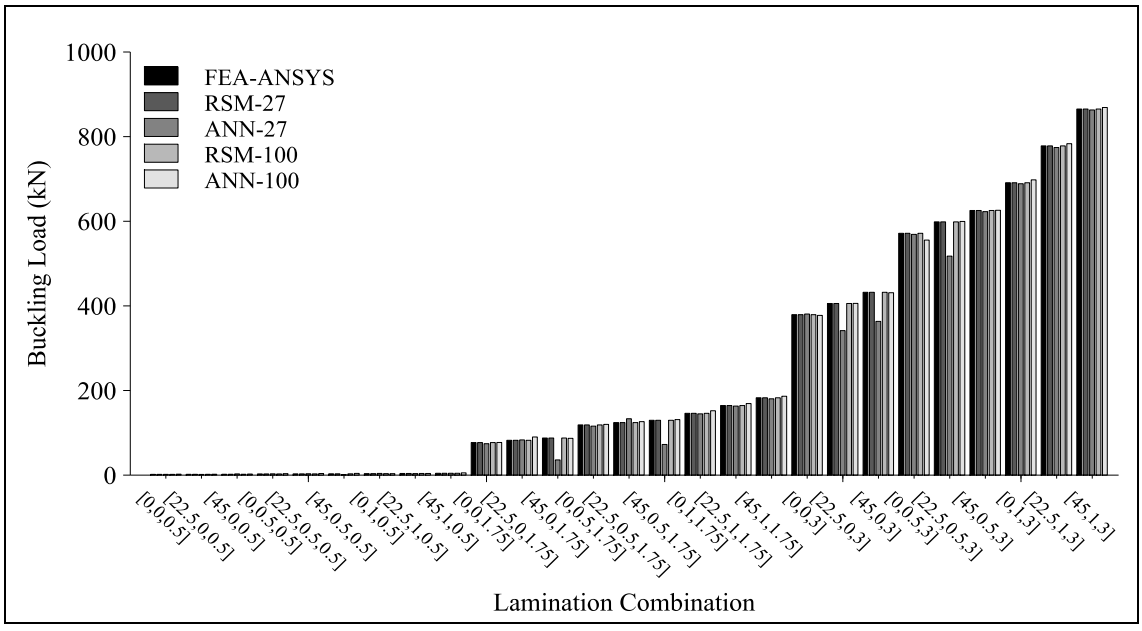

Fig. 18. Comparison of predicted buckling loads from ANSYS, RSM and ANN models.

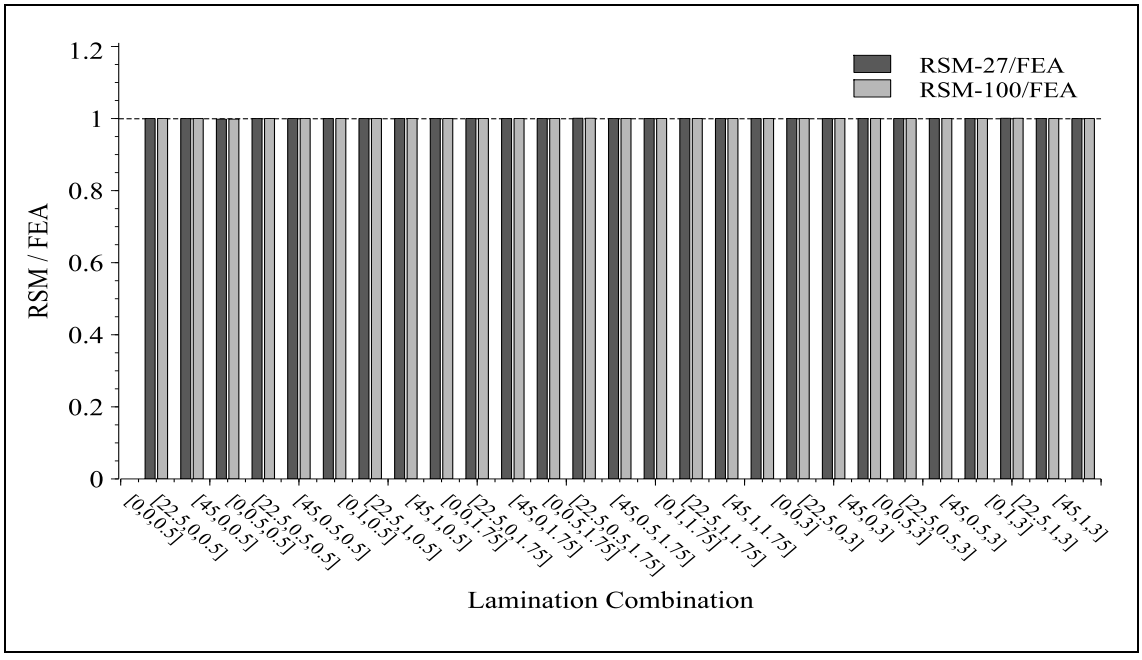

Fig. 19. Summary of predicted buckling loads from ANSYS and RSM models.

https://doi.org/10.24191/jmeche.v23i1.9426

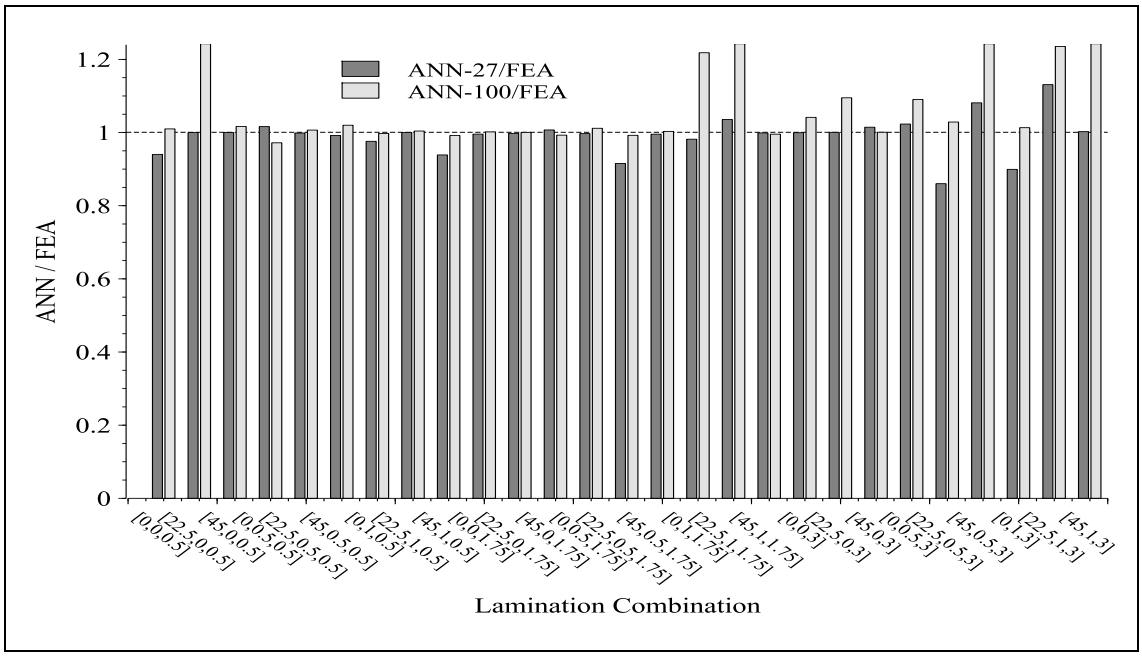

Fig. 20. Summary of predicted buckling loads from ANSYS and ANN models.

Error prediction in comparison to past studies

Table 10 compares the maximum percentage prediction errors for RSM and ANN models from previous studies with those obtained in the current work. The listed errors represent the highest deviation between predicted and actual values reported in each study. In the present study, the RSM model recorded a maximum error of 27.9%, while the ANN model showed 37.9%. These values fall within the ranges of past studies, where RSM errors varied between 2.7% and 887.5% and ANN errors between 1.1% and 428%. Although the current study's error values are not the lowest among those reported, they remain well within the acceptable range, confirming that both the RSM and ANN models demonstrated comparable prediction accuracy to those developed in past studies.

Table 10. Maximum percentage error in modified RSM and ANN models on specific datasets from present and previous studies

Author	RSM max error (%)	ANN max error (%)	Observation / Note
Sadeghpour & Ozay (2025)	887.5	175	Highest errors in RSM among literature
Saaidia et al. (2023)	213.6	1.1	The lowest errors in ANN among literature
Golbaz et al. (2022)	147.3	137.5	Both models errors above 100%
Mahdevari & Hayati (2021)	140	-	ANN not reported
Saada et al. (2023)	107.4	92.8	Both models errors above 90%
Ciğeroğlu et al. (2021)	83	428	The highest errors in ANN among literature
Bello et al. (2024)	60	-	ANN not reported
Nwobi-Okoye et al. (2020)	50	58	Moderate performance for both models
Present Study	27.9	37.9	Within acceptable range based on literature
Wang et al. (2022)	12.7	40.8	ANN slightly less accurate
Ganapathy et al. (2021)	2.7	102	Lowest errors in RSM among literature

https://doi.org/10.24191/jmeche.v23i1.9426

T-test results for dataset consistency

A t-test was conducted using an online calculator to compare the mean outputs between the 27 and 100 datasets for each predictive model type, as shown in Table 11. The test was performed with a significance level of 0.05 and a one-tailed hypothesis to assess whether one case consistently produced higher or lower results than the other. The summary of the t-test results in Table 12 shows that none of the comparisons reached statistical significance at the 0.05 level. This indicates that the models were robust to variations in dataset size and maintained consistent prediction performance, as reported by Martinović et al. (2025). Similar findings were presented by Rainio et al. (2024) in their study on lung infection and tumour detection using datasets of 64 and 128 samples, which also showed no significant differences. Rajput et al. (2023) further supported that dataset size does not strongly influence machine learning performance. Overall, the results suggest that model accuracy depended more on the modelling approach and data treatment rather than dataset size.

Table 11. Descriptive statistic

Group	N	Mean	Sum of squares (SS)	Variance (S^2)
RSM-27	27	480.48	7973184.44	306660.94
RSM-100	100	524.77	21953041.49	221747.89
ANN-27	27	455.59	7685297.16	295588.35
ANN-100	100	522.94	21780906.36	220009.16

Table 12. Independent samples t-test summary

Group comparison	t-value	p-value	Significant ($p < 0.05$)?
RSM-27 and RSM-100	-0.41742	0.338544	No
ANN-27 and ANN-100	-0.63959	0.261803	No

CONCLUSION

Predicting the buckling load of hybrid composite laminates poses significant challenges due to the intricate nonlinear interactions among material properties, geometric parameters, and loading conditions, particularly when relying on limited datasets. This study effectively addressed these challenges by integrating FEA with refined RSM and ANN models, employing dataset sizes of 27 and 100 experimental runs to evaluate predictive accuracy. Through model refinements, such as modified fifth-order polynomial regression in RSM and min-max data normalisation in ANN, the research demonstrated enhanced prediction capabilities while minimising computational and experimental demands. This approach not only validates the buckling behaviour of hybrid graphite/glass epoxy laminates under uniaxial compressive loading but also highlights the potential for cost-effective modelling in composite design, reducing the traditional reliance on extensive datasets or thousands of simulations/experiments.

The key findings are summarized as follows:

- Mesh convergence analysis revealed stabilisation at a 16 × 16 mesh size, with a 20 × 20 mesh selected for optimal balance between computational efficiency and accuracy, aligning with prior studies that emphasize avoiding excessive refinement to prevent unnecessary increases in simulation time.
- FEA model validation against CLPT and HSDT benchmarks yielded percentage errors ranging from 0.001% to 0.23%, confirming the reliability of the ANSYS-based simulations in capturing shear deformation effects and anisotropic material behaviour.

https://doi.org/10.24191/jmeche.v23i1.9426

- Computed buckling loads spanned from 3.627 kN to 1730.8 kN, with the highest values observed at configurations of [45°, 1, 3 mm] (angle, volume fraction, thickness) for full graphite laminates and [45°, 0.5, 3 mm] for hybrid variants, underscoring the synergistic effects of optimized fibre orientation, graphite volume fraction, and plate thickness.
- Plate thickness had the strongest effect on buckling, followed by graphite volume fraction, while fibre orientation had moderate impact. The interaction between thickness and volume fraction was most significant and resulted in increased stiffness and delayed buckling, whereas orientation-volume fraction interactions were weak.
- RSM models (RSM-27 and RSM-100) exhibited superior consistency, with predicted-to-FEA buckling load ratios closely approach unity, which indicates high fidelity, and demonstrated robustness through high R^2 values (near 1), normal residual distributions, and significant ANOVA results (p-values < 0.0002).
- Maximum prediction errors were 27.9% for RSM and 37.9% for ANN, falling well within the ranges reported in literature (RSM: 2.7%–887.5%; ANN: 1.1%–428%), affirming the models' comparability to established benchmarks despite using smaller datasets.
- Independent samples t-test results indicated no statistically significant differences ($p > 0.05$) in mean outputs between the 27- and 100-run datasets for both RSM and ANN, which suggests that refined modelling techniques and data treatment (e.g., normalisation and term reduction) are more critical to accuracy than dataset expansion alone. This thereby enables efficient predictions with reduced resource requirements.

It can be concluded that refined RSM and ANN can achieve reliable buckling predictions for hybrid laminates using modest datasets, potentially saving substantial time and costs in aerospace, automotive, and marine applications where material hybridisation is pursued for performance-cost optimisation. The study bridges existing research gaps in data normalisation for ANN and modified regression in RSM, particularly for small-sample scenarios, and provides practical insights into factor interactions that can guide laminate design. Future work could extend this framework to incorporate additional variables such as environmental effects or dynamic loading, explore hybrid RSM-ANN integrations, or validate predictions through physical experiments to further enhance model generalizability and real-world applicability.

ACKNOWLEDGEMENTS/ FUNDING

The authors would like to express their gratitude to Universiti Teknologi MARA and the Ministry of Higher Education (MOHE), Malaysia for funding the study under the Fundamental Research Grant Scheme (FRGS) FRGS/1/2023/TK10/UITM/02/3 and UiTM file number 600-RMC/FRGS 5/3 (001/2023).

CONFLICT OF INTEREST STATEMENT

The authors agree that this research was conducted in the absence of any self-benefits, commercial or financial conflicts and declare the absence of conflicting interests with the funders.

https://doi.org/10.24191/jmeche.v23i1.9426

AUTHORS' CONTRIBUTIONS

The authors confirm their contribution to the paper as follows: conceptualisation: Muhammad Naufal Mohd Najib, Azizul Hakim Samsudin, Mohd Shahrom Ismail, Jamaluddin Mahmud; simulation: Muhammad Naufal Mohd Najib; data collection: Muhammad Naufal Mohd Najib; analysis: Muhammad Naufal Mohd Najib, Mohd Shahrom Ismail; writing—original draft: Muhammad Naufal Mohd Najib; writing—review and editing: Azizul Hakim Samsudin, Mohd Shahrom Ismail, Chi Hieu Le, Ho Quang Nguyen, Jamaluddin Mahmud; data verification: Mohd Shahrom Ismail, Jamaluddin Mahmud; finalising: Mohd Shahrom Ismail, Chi Hieu Le, Ho Quang Nguyen, Jamaluddin Mahmud; supervision: Azizul Hakim Samsudin, Jamaluddin Mahmud (main supervision); funding: Azizul Hakim Samsudin (research grant leader), Jamaluddin Mahmud (research grant member). All authors reviewed the results and approved the final version of the manuscript.

REFERENCE

Achour, B., Ouinas, D., Touahmia, M., & Boukendakdji, M. (2018). Buckling of hybrid composite carbon/epoxy/aluminum plates with cutouts. Engineering, Technology & Applied Science Research, 8(1), 2393–2398.

Adizue, U. L., & Takács, M. (2025). Exploring the correlation between design of experiments and machine learning prediction accuracy in ultra-precision hard turning of AISI D2 with CBN insert: a comparative study of Taguchi and full factorial designs. International Journal of Advanced Manufacturing Technology, 137(3-4), 2061–2090.

Afaq, S., & Rao, S. (2020). Significance of epochs on training a neural network. International Journal of Scientific & Technology Research, 9(6), 485–488.

Aghelpour, P., Bagheri-Khalili, Z., Varshavian, V., & Mohammadi, B. (2022). Evaluating three supervised machine learning algorithms (LM, BR, and SCG) for daily pan evaporation estimation in a semi-arid region. Water, 14(21), 3435.

Aksu, G., Guzeller, C. O., & Eser, M. T. (2019). The effect of the normalization method used in different sample sizes on the success of artificial neural network model. International Journal of Assessment Tools in Education, 6(2), 170–192.

Alam, M. A., Ya, H. H., Azeem, M., Hussain, P., Salit, M. S., Khan, R., Arif, S., & Ansari, A. H. (2020). Modelling and optimisation of hardness behaviour of sintered Al/SiC composites using RSM and ANN: a comparative study. Journal of Materials Research and Technology, 9(6), 14036–14050.

Alhawamdeh, M., Alajarmeh, O., Aravinthan, T., Shelley, T., Schubel, P., Mohammed, A., & Zeng, X. (2021). Review on local buckling of hollow box FRP profiles in civil structural applications. Polymers, 13(23), 4159.

Bakamal, A., Ansari, R., & Hassanzadeh-Aghdam, M. K. (2021a). Bending, free vibration, and buckling responses of chopped carbon fiber/graphene nanoplatelet-reinforced polymer hybrid composite plates: an inclusive microstructural assessment. Proceedings of the Institution of Mechanical Engineers, Part C: Journal of Mechanical Engineering Science, 235(8), 1455–1469.

Bakamal, A., Ansari, R., & Hassanzadeh-Aghdam, M. K. (2021b). Computational analysis of the effects of carbon nanotubes on the bending, buckling, and vibration characteristics of carbon fabric/polymer hybrid nanocomposite plates. Journal of the Brazilian Society of Mechanical Sciences and Engineering, 43(2), 61.

https://doi.org/10.24191/jmeche.v23i1.9426

Barnett, P. R., Hmeidat, N. S., Zheng, B., & Penumadu, D. (2024). Toward a circular economy: zero-waste manufacturing of carbon fiber-reinforced thermoplastic composites. npj Materials Sustainability, 2, 3.

Bello, U., Amran, N. A., Hazwan Ruslan, M. S., Yáñez, E. H., Suparmaniam, U., Adamu, H., Abba, S. I., Tafida, U. I., & Mahmoud, A. A. (2024). Enhancing oxidative stability of biodiesel using fruit peel waste extracts blend: comparison of predictive modelling via RSM and ANN techniques. Results in Engineering, 21, 101853.

Bijjam, R. R., Chandanam, S., Nakka, V. V. S. S., & Dhoria, S. H. (2023). Stress analysis in a multiscale composite laminated plate with cutout at the centre using finite element method. Annales de Chimie : Science Des Materiaux, 47(6), 393–398.

Boukarma, L., Aboussabek, A., El Aroussi, F., Zerbet, M., Sinan, F., & Chiban, M. (2023). Insight into mechanism, Box-Behnken design, and artificial neural network of cationic dye biosorption by marine macroalgae Fucus spiralis. Algal Research, 76, 103324.

Can, Ö., Baklacioglu, T., Özturk, E., & Turan, O. (2022). Artificial neural networks modeling of combustion parameters for a diesel engine fueled with biodiesel fuel. Energy, 247, 123473.

Chakravarty, S., Demirhan, H., & Baser, F. (2020). Fuzzy regression functions with a noise cluster and the impact of outliers on mainstream machine learning methods in the regression setting. Applied Soft Computing, 96, 106535.

Ciğeroğlu, Z., Küçükyıldız, G., Erim, B., & Alp, E. (2021). Easy preparation of magnetic nanoparticles-rGO-chitosan composite beads: optimization study on cefixime removal based on RSM and ANN by using Genetic Algorithm Approach. Journal of Molecular Structure, 1224, 129182.

Damghani, M., Pir, R. A., Murphy, A., & Fotouhi, M. (2022). Experimental and numerical study of hybrid (CFRP-GFRP) composite laminates containing circular cut-outs under shear loading. Thin-Walled Structures, 179, 109752.

Damghani, M., Wallis, C., Bakunowicz, J., & Murphy, A. (2021). Using laminate hybridisation (CFRP-GFRP) and shaped CFRP plies to increase plate post-buckling strain to failure under shear loading. Thin-Walled Structures, 162, 107543.

Dogan, A. (2020). Buckling analysis of laminated composite plates under the effect of uniaxial and biaxial loads. Turkish Journal of Engineering, 4(4), 218–225.

Ertugrul, G., Hälsig, A., Rimpl, R., Hensel, J., & Härtel, S. (2025). Artificial neural network based calibration of goldek heat source parameters in tandem plasma transferred arc process using finite element analysis. International Journal of Advanced Manufacturing Technology, 139(5-6), 2349–2363.

Evran, S. (2020). Numerical and statistical buckling analysis of laminated composite plates with functionally graded fiber orientation angles. Polymers and Polymer Composites, 28(7), 502–512.

Fan, C., Chen, M., Wang, X., Wang, J., & Huang, B. (2021). A review on data preprocessing techniques toward efficient and reliable knowledge discovery from building operational data. Frontiers in Energy Research, 9, 652801.

Feng, C., Li, L., & Sadeghpour, A. (2020). A comparison of residual diagnosis tools for diagnosing regression models for count data. BMC Medical Research Methodology, 20(1), 175.

Ganapathy, S., Balasubramanian, P., Vasanth, B., & Thulasiraman, S. (2021). Comparative investigation of Artificial Neural Network (ANN) and Response Surface Methodology (RSM) expectation in EDM parameters. Materials Today: Proceedings, 46(19), 9592–9596.

https://doi.org/10.24191/jmeche.v23i1.9426

Goel, M. D., Bedon, C., Singh, A., Khatri, A. P., & Gupta, L. M. (2021). An abridged review of buckling analysis of compression members in construction. Buildings, 11(5), 211.

Golbaz, S., Nabizadeh, R., Rafiee, M., & Yousefi, M. (2022). Comparative study of RSM and ANN for multiple target optimisation in coagulation/precipitation process of contaminated waters: mechanism and theory. International Journal of Environmental Analytical Chemistry, 102(19), 8519–8537.

Gopalan, V., Suthenthiraveerappa, V., David, J. S., Subramanian, J., Raja Annamalai, A., & Jen, C. P. (2021). Experimental and numerical analyses on the buckling characteristics of woven flax/epoxy laminated composite plate under axial compression. Polymers, 13(7), 995.

Gukop, N. S., Kamtu, P. M., Lengs, B. D., Babawuya, A., & Adegoke, A. (2021). Effect of mesh density on finite element analysis simulation of a support bracket. Journal of Engineering and Technology, 6(3), 34–38.

Hajduk, Z., & Dec, G. R. (2023). Very high accuracy hyperbolic tangent function implementation in FPGAs. IEEE Access, 11, 23701–23713.

Han, H., & Dong, C. (2024). Buckling analysis for carbon and glass fibre reinforced hybrid composite stiffened panels. Journal of Composites Science, 8(1), 34.

Hemmat, M., Toghraie, D., & Amoozad, F. (2023). Prediction of viscosity of MWCNT-Al2O3 (20:80)/SAE40 nano-lubricant using multi-layer artificial neural network (MLP-ANN) modeling. Engineering Applications of Artificial Intelligence, 121, 105948.

Ho-Huu, V., Do-Thi, T. D., Dang-Trung, H., Vo-Duy, T., & Nguyen-Thoi, T. (2016). Optimization of laminated composite plates for maximizing buckling load using improved differential evolution and smoothed finite element method. Composite Structures, 146, 132–147.

Hsissou, R., Seghiri, R., Benzekri, Z., Hilali, M., Rafik, M., & Elharfi, A. (2021). Polymer composite materials: a comprehensive review. Composite Structures, 262, 113640.

Jha, A. K., & Sit, N. (2021). Comparison of response surface methodology (RSM) and artificial neural network (ANN) modelling for supercritical fluid extraction of phytochemicals from Terminalia chebula pulp and optimization using RSM coupled with desirability function (DF) and genetic algorithm (GA) and ANN with GA. Industrial Crops and Products, 170, 113769.

Joshi, S. V., Drzal, L. T., Mohanty, A. K., & Arora, S. (2004). Are natural fiber composites environmentally superior to glass fiber reinforced composites? Composites Part A: Applied Science and Manufacturing, 35(3), 371–376.

Kamarudin, M. N., Mohamed Ali, J. S., Aabid, A., & Ibrahim, Y. E. (2022). Buckling analysis of a thin-walled structure using finite element method and design of experiments. Aerospace, 9(10), 541.

Khelifa, H., Bezazi, A., Boumediri, H., delPino, G. G., Ellagoune, S., Reis, P. N. B., & Scarpa, F. (2025). Mechanical properties optimization using response surface methodology (RSM) of a bio-mortar manufactured based on sisal fibers. International Journal of Advanced Manufacturing Technology, 138(5-6), 2335–2355.

Kumar, V., Kedam, N., Sharma, K. V., Mehta, D. J., & Caloiero, T. (2023). Advanced machine learning techniques to improve hydrological prediction: a comparative analysis of streamflow prediction models. Water, 15(14), 2572.

Kumar, P. R., Gupta, G., Shamili, G. K., & Anitha, D. (2018). Linear buckling analysis and comparative study of un-stiffened and stiffened composite plate. Materials Today: Proceedings, 5(2), 6059–6071.

https://doi.org/10.24191/jmeche.v23i1.9426

Lee, B. C. Y., Mahtab, M. S., Neo, T. H., Farooqi, I. H., & Khursheed, A. (2022). A comprehensive review of design of experiment (DOE) for water and wastewater treatment application - key concepts, methodology and contextualized application. Journal of Water Process Engineering, 47, 102673.

Leishman, J. G. (2023). Aerospace structures. Introduction to aerospace flight vehicles (pp. 327–362). Embry-Riddle Aeronautical University.

Li, D. M., Featherston, C. A., & Wu, Z. (2020). An element-free study of variable stiffness composite plates with cutouts for enhanced buckling and post-buckling performance. Computer Methods in Applied Mechanics and Engineering, 371, 113314.

Liu, X., Qin, J., Zhao, K., Featherston, C. A., Kennedy, D., Jing, Y., & Yang, G. (2023). Design optimization of laminated composite structures using artificial neural network and genetic algorithm. Composite Structures, 305, 116500.

Long, S., Chen, C., Wang, H., Yao, X., & Zhang, X. (2022). Distribution and propagation of matrix cracks within composite laminates under impact. Composite Structures, 281, 115005.

Mahdevari, S., & Hayati, M. (2021). Finite-difference based response surface methodology to optimize tailgate support systems in longwall coal mining. Scientific Reports, 11, 2321.

Malekjani, N., & Jafari, S. M. (2020). Food process modeling and optimization by response surface methodology (RSM). In S. Surajbhan & A. Singh (Eds.), Mathematical and statistical applications in food engineering (1st Ed., pp. 181–203). CRC Press.

Mamun, A. A., Sohel, M., Mohammad, N., Sunny, M. S. H., Dipta, D. R., & Hossain, E. (2020). A comprehensive review of the load forecasting techniques using single and hybrid predictive models. IEEE Access, 8, 134911– 134939.

Martinović, M., Dokic, K., & Pudić, D. (2025). Comparative analysis of machine learning models for predicting innovation outcomes: an applied AI approach. Applied Sciences, 15(7), 3636.

Nwobi-Okoye, C. C., Anyichie, M. K., & Atuanya, C. U. (2020). RSM and ANN modeling for production of Newbouldia Laevies Fibre and recycled high density polyethylene composite: multi objective optimization using genetic algorithm. Fibers and Polymers, 21(4), 898–909.

Okereke, M., & Keates, S. (2018). Finite element mesh generation. Finite element applications (pp. 165–186). Springer.

Okpalaeke, K. E., Ibrahim, T. H., Latinwo, L. M., & Betiku, E. (2020). Mathematical modeling and optimization studies by artificial neural network, genetic algorithm and response surface methodology: a case of ferric sulfate–catalyzed esterification of neem (Azadirachta indica) seed oil. Frontiers in Energy Research, 8, 614621.

Oza, S., Kodgire, P., & Kachhwaha, S. S. (2022). Analysis of RSM based BBD and CCD techniques applied for biodiesel production from waste cotton-seed cooking oil via ultrasound method. Analytical Chemistry Letters, 12(1), 86–101.

Phan, N. D., & Reddy, J. N. (1985). Analysis of laminated composite plates using a higher-order shear deformation theory. International Journal for Numerical Methods in Engineering, 21(12), 2201–2219.

Ponticelli, M., Carlucci, V., Mecca, M., Todaro, L., Milella, L., & Russo, D. (2024). Extraction optimization of Quercus cerris L. wood chips: a comparative study between full factorial design (FFD) and artificial neural network (ANN). Antioxidants, 13(9), 1115.

https://doi.org/10.24191/jmeche.v23i1.9426

Rainio, O., Teuho, J., & Klén, R. (2024). Evaluation metrics and statistical tests for machine learning. Scientific Reports, 14(1), 6086.

Rajak, D. K., Wagh, P. H., & Linul, E. (2021). Manufacturing technologies of carbon/glass fiber-reinforced polymer composites and their properties: a review. Polymers, 13(21), 3721.

Rajput, D., Wang, W. J., & Chen, C. C. (2023). Evaluation of a decided sample size in machine learning applications. BMC Bioinformatics, 24(1), 48.

Reji, M., & Kumar, R. (2022). Response surface methodology (RSM): an overview to analyze multivariate data. Indian Journal of Microbiology Research, 9(4), 241–248.

Revanesh, M., Gundal, S. S., Arunkumar, J. R., Josephson, P. J., Suhasini, S., & Devi, T. K. (2024). Artificial neural networks-based improved Levenberg–Marquardt neural network for energy efficiency and anomaly detection in WSN. Wireless Networks, 30(6), 5613–5628.

Rostamijavanani, A., Ebrahimi, M. R., & Jahedi, S. (2021). Thermal post-buckling analysis of laminated composite plates embedded with shape memory alloy fibers using semi-analytical finite strip method. Journal of Failure Analysis and Prevention, 21(1), 290–301.

Roy, R. B., Rokonuzzaman, M., Amin, N., Mishu, M. K., Alahakoon, S., Rahman, S., Mithulananthan, N., Rahman, K. S., Shakeri, M., & Pasupuleti, J. (2021). A comparative performance analysis of ANN algorithms for MPPT energy harvesting in solar PV system. IEEE Access, 9, 102137–102152.

Saada, K., Amroune, S., & Zaoui, M. (2023). Prediction of mechanical behavior of epoxy polymer using artificial neural networks (ANN) and response surface methodology (RSM). Fracture and Structural Integrity, 17(66), 191–206.

Saaidia, A., Belaadi, A., Boumaaza, M., Alshahrani, H., & Bourchak, M. (2023). Effect of water absorption on the behavior of jute and sisal fiber biocomposites at different lengths: ANN and RSM modeling. Journal of Natural Fibers, 20(1), 2140326.

Sadeghpour, A., & Ozay, G. (2025). Investigating the predictive capabilities of ANN, RSM, and ANFIS in assessing the collapse potential of RC structures. Arabian Journal for Science and Engineering, 50(16), 13169–13190.

Saha, S., Mondal, A. K., Čep, R., Joardar, H., Haldar, B., Kumar, A., Alsalah, N. A., & Ataya, S. (2024). Multi-response optimization of electrochemical machining parameters for Inconel 718 via RSM and MOGA-ANN. Machines, 12(5), 335.

Santhosh, A. J., Tura, A. D., Jiregna, I. T., Gemechu, W. F., Ashok, N., & Ponnusamy, M. (2021). Optimization of CNC turning parameters using face centred CCD approach in RSM and ANN-genetic algorithm for AISI 4340 alloy steel. Results in Engineering, 11, 100251.

Sarker, I. H. (2021). Machine learning: algorithms, real-world applications and research directions. SN Computer Science, 2(3), 160.

Schilling, J. C., & Mittelstedt, C. (2025). Closed-form postbuckling analysis of shear-deformable composite laminated panels. Archive of Applied Mechanics, 95(1), 17.

Shokri, A., Moradi, H., Abdouss, M., & Nasernejad, B. (2020). Employing UV/periodate process for degradation of p-chloronitrobenzene in aqueous environment. Desalination and Water Treatment, 205, 264–274.

Sibiya, N. P., Amo-Duodu, G., Tetteh, E. K., & Rathilal, S. (2022). Model prediction of coagulation by

https://doi.org/10.24191/jmeche.v23i1.9426

magnetised rice starch for wastewater treatment using response surface methodology (RSM) with artificial neural network (ANN). Scientific African, 17, e01282.

Silva, A. R., Ayuso, M., Oludemi, T., Gonçalves, A., Melgar, B., & Barros, L. (2024). Response surface methodology and artificial neural network modeling as predictive tools for phenolic compounds recovery from olive pomace. Separation and Purification Technology, 330(A), 125351.

Silva, G. H. C., & Meddaikar, Y. (2020). Lamination parameters for sandwich and hybrid material composites. AIAA Journal, 58(10), 4604–4611.

Suriani, M. J., Rapi, H. Z., Ilyas, R. A., Petrů, M., & Sapuan, S. M. (2021). Delamination and manufacturing defects in natural fiber-reinforced hybrid composite: a review. Polymers, 13(8), 1323.

Szpisják-Gulyás, N., Al-Tayawi, A. N., Horváth, Z. H., László, Z., Kertész, S., & Hodúr, C. (2023). Methods for experimental design, central composite design and the Box–Behnken design, to optimise operational parameters: a review. Acta Alimentaria, 52(4), 521–537.

Thakur, A., & Konde, A. (2021). Fundamentals of neural networks. International Journal for Research in Applied Science and Engineering Technology, 9(8), 407–426.

Wang, B., Ma, X., Tian, K., Hao, P., Zhou, Y., & Quan, D. (2019). Concurrent patch optimization of hybrid composite plates based on proper orthogonal decomposition. AIAA Journal, 57(11), 4915–4926.

Wang, K., Mao, Y., Wang, C., Ke, Q., Zhao, M., & Wang, Q. (2022). Application of a combined response surface methodology (RSM)-artificial neural network (ANN) for multiple target optimization and prediction in a magnetic coagulation process for secondary effluent from municipal wastewater treatment plants. Environmental Science and Pollution Research International, 29(24), 36075–36087.

Wankhade, R. L., & Niyogi, S. B. (2020). Buckling analysis of symmetric laminated composite plates for various thickness ratios and modes. Innovative Infrastructure Solutions, 5(3), 65.

Xiao, Z., & Harrison, P. (2021). Design of buckling and damage resistant steered fibre composite laminates using trellis shear kinematics. Composite Structures, 260, 113526.

Yang, Y., Wu, B., Xu, L. Y., Yao, Y. P., Zhang, D., & Zhao, C. (2022). Experimental study on the buckling behavior of double steel plate concrete composite slabs with stiffening ribs and tie plates. Engineering Structures, 255, 113895.

Yang, Z., Cao, Y., & Liu, J. (2021). A buckling analysis and optimization method for a variable stiffness cylindrical pressure shell of AUV. Journal of Marine Science and Engineering, 9(6), 637.

Zhang, J., Lin, G., Yin, X., Zeng, J., Wen, S., & Lan, Y. (2020). Application of artificial neural network (ANN) and response surface methodology (RSM) for modeling and optimization of the contact angle of rice leaf surfaces. Acta Physiologiae Plantarum, 42(4), 51.

Zhang, Y., Cao, P., Yang, X., & Niu, K. (2025). Buckling modeling and numerical validation of composite panels for sandwich structures. Journal of Sandwich Structures & Materials, 27(6), 1195-1219.

https://doi.org/10.24191/jmeche.v23i1.9426

APPENDIX

A. Buckling load from ANSYS for 100 experimental runs

Run	Angle of Orientation (°)	Volume Fraction	Plate Thickness (mm)	FEA-ANSYS (kN)
1	45	1	3	1730.8
2	22.5	0.5	1.75	248.72
3	22.5	0.5	1.75	248.72
4	22.5	0.5	1.75	248.72
5	22.5	0.5	1.75	248.72
6	22.5	0.5	1.75	248.72
7	22.5	0.5	1.75	248.72
8	22.5	0.5	1.75	248.72
9	22.5	0.5	1.75	248.72
10	22.5	0.5	1.75	248.72
11	22.5	0.5	1.75	248.72
12	22.5	0.5	1.75	248.72
13	22.5	0.5	1.75	248.72
14	22.5	0.5	1.75	248.72
15	22.5	1	3	1555.8
16	45	0.875	3	1521.2
17	45	0.75	3	1391.9
18	0	1	3	1382.2
19	45	0.625	3	1301.9
20	45	0.5	3	1251.3
21	45	0.25	3	1250.5
22	45	0.375	3	1249.6
23	40.5	0.5	3	1248.1
24	36	0.5	3	1240.1
25	31.5	0.5	3	1228.1
26	27	0.5	3	1213
27	22.5	0.5	3	1196.5
28	18	0.5	3	1180
29	13.5	0.5	3	1165.2
30	9	0.5	3	1153.5
31	4.5	0.5	3	1146
32	0	0.5	3	1143.4
33	45	0.125	3	1006.1
34	45	0.5	2.75	973.52
35	40.5	0.5	2.75	971.13
36	36	0.5	2.75	964.99
37	31.5	0.5	2.75	955.65
38	27	0.5	2.75	943.99
39	22.5	0.5	2.75	931.15
40	18	0.5	2.75	918.35
41	13.5	0.5	2.75	906.85
42	9	0.5	2.75	897.74
43	4.5	0.5	2.75	891.9
44	0	0.5	2.75	889.89

https://doi.org/10.24191/jmeche.v23i1.9426

45	45	0	3	864.33
46	22.5	0	3	811.23
47	0	0	3	758.56
48	45	0.5	2.5	738.22
49	45	0.5	2.25	542.73
50	45	0.5	2	384.1
51	40.5	0.5	2	383.25
52	36	0.5	2	380.9
53	31.5	0.5	2	377.27
54	27	0.5	2	372.72
55	22.5	0.5	2	367.69
56	45	1	1.75	365.61
57	18	0.5	2	362.67
58	13.5	0.5	2	358.15
59	9	0.5	2	354.56
60	4.5	0.5	2	352.27
61	0	0.5	2	351.47
62	22.5	1	1.75	328.84
63	0	1	1.75	292.2
64	45	0.5	1.75	259.07
65	22.5	0.5	1.75	248.72
66	0	0.5	1.75	237.14
67	45	0	1.75	175.47
68	22.5	0	1.75	164.65
69	45	0.5	1.5	164.12
70	0	0	1.75	153.89
71	45	0.5	1.25	95.456
72	40.5	0.5	1.25	95.259
73	36	0.5	1.25	94.688
74	31.5	0.5	1.25	93.798
75	27	0.5	1.25	92.675
76	22.5	0.5	1.25	91.432
77	18	0.5	1.25	90.189
78	13.5	0.5	1.25	89.069
79	9	0.5	1.25	88.181
80	4.5	0.5	1.25	87.611
81	0	0.5	1.25	87.415
82	45	0.5	1	49.077
83	45	0.5	0.75	20.772
84	45	1	0.5	8.7967
85	22.5	0.5	1.75	248.72
86	22.5	0.5	1.75	248.72
87	45	0.5	0.5	6.1688
88	40.5	0.5	0.5	6.1567
89	22.5	0.5	1.75	248.72
90	22.5	0.5	1.75	248.72
91	27	0.5	0.5	5.9909
92	22.5	0.5	0.5	5.9109
93	18	0.5	0.5	5.8306
94	13.5	0.5	0.5	5.7584

https://doi.org/10.24191/jmeche.v23i1.9426

95	9	0.5	0.5	5.7011
96	4.5	0.5	0.5	5.6643
97	22.5	0.5	1.75	248.72
98	22.5	0.5	1.75	248.72
99	22.5	0.5	1.75	248.72
100	0	0	0.5	3.627

B. *Predicted Buckling Load from ANSYS, RSM and ANN Models for 100 experimental runs*

FEA-ANSYS (A)	Response (kN)		Error Percentage (%)	
	RSM-100 (B)	ANN-100 (C)	|A – B| / A x 100	|A – C| / A x 100
1730.8	1730.57	1737.71	0.0	0.4
248.72	248.31	252.86	0.2	1.7
248.72	248.31	252.86	0.2	1.7
248.72	248.31	252.86	0.2	1.7
248.72	248.31	252.86	0.2	1.7
248.72	248.31	252.86	0.2	1.7
248.72	248.31	252.86	0.2	1.7
248.72	248.31	252.86	0.2	1.7
248.72	248.31	252.86	0.2	1.7
248.72	248.31	252.86	0.2	1.7
248.72	248.31	252.86	0.2	1.7
248.72	248.31	252.86	0.2	1.7
248.72	248.31	252.86	0.2	1.7
248.72	248.31	252.86	0.2	1.7
1555.8	1556.27	1566.72	0.0	0.7
1521.2	1601.99	1523.71	5.3	0.2
1391.9	1479.20	1393.48	6.3	0.1
1382.2	1381.97	1395.73	0.0	1.0
1301.9	1362.21	1306.26	4.6	0.3
1251.3	1251.02	1252.03	0.0	0.1
1250.5	1046.04	1248.57	16.4	0.2
1249.6	1145.63	1250.30	8.3	0.1
1248.1	1240.23	1246.67	0.6	0.1
1240.1	1229.44	1239.25	0.9	0.1
1228.1	1218.65	1228.19	0.8	0.0
1213	1207.86	1214.55	0.4	0.1
1196.5	1197.07	1199.18	0.0	0.2
1180	1186.28	1182.94	0.5	0.2
1165.2	1175.49	1166.01	0.9	0.1
1153.5	1164.70	1148.40	1.0	0.4
1146	1153.91	1130.26	0.7	1.4
1143.4	1143.12	1111.09	0.0	2.8
1006.1	952.25	1005.21	5.4	0.1
973.52	993.58	976.72	2.1	0.3
971.13	985.03	973.09	1.4	0.2
964.99	976.47	966.35	1.2	0.1
955.65	967.92	956.68	1.3	0.1
943.99	959.36	945.45	1.6	0.2
931.15	950.81	933.88	2.1	0.3

https://doi.org/10.24191/jmeche.v23i1.9426

918.35	942.26	922.31	2.6	0.4
906.85	933.70	910.57	3.0	0.4
897.74	925.15	898.30	3.1	0.1
891.9	916.59	885.52	2.8	0.7
889.89	908.04	871.88	2.0	2.0
864.33	864.26	862.20	0.0	0.2
811.23	811.38	811.77	0.0	0.1
758.56	758.49	755.12	0.0	0.5
738.22	765.69	743.55	3.7	0.7
542.73	567.34	548.20	4.5	1.0
384.1	398.53	388.61	3.8	1.2
383.25	395.14	388.79	3.1	1.4
380.9	391.74	386.37	2.8	1.4
377.27	388.35	382.40	2.9	1.4
372.72	384.95	378.08	3.3	1.4
367.69	381.56	373.24	3.8	1.5
365.61	365.59	372.90	0.0	2.0
362.67	378.16	368.41	4.3	1.6
358.15	374.76	363.57	4.6	1.5
354.56	371.37	359.60	4.7	1.4
352.27	367.97	356.49	4.5	1.2
351.47	364.58	354.59	3.7	0.9
328.84	328.89	338.35	0.0	2.9
292.2	292.18	304.33	0.0	4.2
259.07	259.28	262.53	0.1	1.3
248.72	248.31	252.86	0.2	1.7
237.14	237.35	239.90	0.1	1.2
175.47	175.46	174.01	0.0	0.8
164.65	164.67	180.32	0.0	9.5
164.12	149.56	166.86	8.9	1.7
153.89	153.88	154.37	0.0	0.3
95.456	69.40	97.62	27.3	2.3
95.259	68.84	98.62	27.7	3.5
94.688	68.27	98.14	27.9	3.6
93.798	67.71	96.72	27.8	3.1
92.675	67.15	94.89	27.5	2.4
91.432	66.59	93.25	27.2	2.0
90.189	66.03	92.01	26.8	2.0
89.069	65.46	91.11	26.5	2.3
88.181	64.90	90.40	26.4	2.5
87.611	64.34	89.86	26.6	2.6
87.415	63.78	89.66	27.0	2.6
49.077	248.31	50.78	0.2	3.5
20.772	248.31	22.47	0.2	8.2
8.7967	8.80	10.72	0.0	21.8
248.72	248.31	252.86	0.2	1.7
248.72	248.31	252.86	0.2	1.7
6.1688	6.17	8.21	0.0	33.2
6.1567	6.12	8.49	0.6	37.9
248.72	248.31	252.86	0.2	1.7
248.72	248.31	252.86	0.2	1.7

https://doi.org/10.24191/jmeche.v23i1.9426

5.9909	5.96	7.99	0.5	33.4
5.9109	5.91	7.65	0.0	29.4
5.8306	5.86	7.32	0.5	25.5
5.7584	5.81	7.11	0.9	23.5
5.7011	5.76	7.09	1.0	24.4
5.6643	5.70	7.27	0.7	28.3
248.72	248.31	252.86	0.2	1.7
248.72	248.31	252.86	0.2	1.7
248.72	248.31	252.86	0.2	1.7
3.627	3.63	4.55	0.0	25.5

https://doi.org/10.24191/jmeche.v23i1.9426